Student thesis series INES nr 440

Climate change impact on water balance and export of dissolved organic carbon

– a sub-catchment modelling approach

Stina Sandgren

2017
Department of
Physical Geography and Ecosystem Science
Lund University
Sölvegatan 12
S-223 62 Lund
Sweden

Stina Sandgren (2017).

Climate change impact on water balance and export of dissolved organic carbon – a sub-catchment modelling approach

Modellering av vattenföring och utlakning av löst organiskt kol i två olika avrinningsområden under ett förändrat klimat
Master degree thesis, 30 credits in *Physical Geography and Ecosystem Analysis*
Department of Physical Geography and Ecosystem Science, Lund University

Level: Master of Science (MSc)

Course duration: *January* 2017 until *June* 2017

Climate change impact on water balance and export of dissolved organic carbon

– a sub-catchment modelling approach

Stina Sandgren

Master thesis, 30 credits, in *Physical Geography and Ecosystem Analysis*

Main supervisor Jörgen Olofsson
Department of Physical Geography and Ecosystem Analysis, Lund University

Assistant supervisor Annemarie Gärdenäs
Department of Biological and Environment Sciences, University of Gothenburg

Exam committee:
Martin Berggren
Department of Physical Geography and Ecosystem Analysis, Lund University
Examiner 2,
Affiliation

Acknowledgements

I would like to thank and extend my sincere gratitude to my supervisors Jörgen Olofsson and Annemaire Reurslag Gärdenäs for thoughtful insights, motivation and clear and concise guiding in the to me fairly new research field. Without your expertise and helpfulness, this project would not have been possible.

I would also like to thank all the people involved in this project by providing data, aspects on methodology and help along the way; Leif Klemedtsson, David Allbrand, Per Weslien, Tinghai Ou, Hongxing He and Lotta Pers.

Least but not least, thank you Martin for all your support. And to all friends and family, in one way or the other mentally involved in the writing process – I owe you a big one.

Abstract

Climate change will alter the hydrological cycle in the 21st century with implications for the water balance and water quality. As characteristics of the landscape may vary significantly between nearby locations, hydrological models need to be able to delineate responses attributed to specific landscape characteristics, to estimate their responses to altered climatic drivers. Small streams are the main carriers of Dissolved Organic Carbon (DOC) originating from the terrestrial landscape, however the mechanisms controlling production and mobilisation are not yet fully scientifically understood.

The Skogaryd research catchment in Sweden was established in 2013 and includes characteristically different sub-catchments where discharge and other abiotic measurements take place at sub-catchment level and at the main catchment outlet. Covering the dynamics of the constituent sub-catchments would facilitate environmental assessments of the large catchments as the respective contribution of runoff and solutes are known.

This study's aims were to 1) model and compare the water balance of two characteristically different sub-catchments; a forest on mineral soil-, and a mire in the Skogaryd research catchment, by means of the hydrological model HYPE, 2) investigate the impact of climate change on the water balance, especially discharge, and 3) quantify DOC export by studying the control on the temporal DOC aquatic-terrestrial connectivity in the two sub-catchments.

The model HYPE (HYdrological Predictions for the Environment) was set-up and calibrated for both catchments. Downscaled regional bias corrected climate data following the climate scenarios RCP2.6, RCP4.5 and RCP8.5 was then applied to the HYPE model. DOC was sampled and then modelled using catchment specific linear regression derived from an Automatic Linear Modelling regression analysis.

The model adequately captured seasonal dynamics in the hydrological regime in spring, winter and autumn but not in summer. The HYPE model simulated a decrease in discharge in the long-term future, which is inconsistent with other model studies. The running mean temperature 60 days prior to sampling could explain 57% and 65% of DOC concentrations for the mire and forest sub-catchment, respectively.

Likely, discharge will alter in the long-term future, there will be a shift towards autumn and winter discharge, whereas snowmelt driven discharge will diminish. Both catchments proved a very strong temperature control to DOC concentrations; however, the model likely captured the production of DOC rather than the mobilisation. Due to the complex interactions, governing DOC production and mobilisation, it was not possible to estimate the effect of climate change on DOC export.

Keywords: HYPE, Hydrological modelling, DOC, Climate change, Water balance, Specific discharge, Hydrology, Climate scenarios, Carbon cycle, Mire catchment, Forest catchment.

Abbreviations

CC = Correlation Coefficient

CO_2 = Carbon dioxide

DOC = Dissolved organic carbon

ET = Evapotranspiration

FC = Forest catchment

GCM = Global Climate Model

HYPE = HYdrological Predictions for the Environment

IPCC = Intergovernmental Panel on Climate Change

MAP = Mean annual precipitation

MAT = Mean annual temperature

MC = Mire catchment

NSE = Nash Sutcliffe Efficiency

P = Precipitation

P1 = Period 1 (1961-1990)

P2 = Period 2 (2071-2100)

PET = Potential evapotranspiration

Q = Discharge (l s^{-1})

q = Discharge (mm d^{-1})

RB = Relative Bias

RCP = Representative concentration pathways

RMSE = Root Mean Square Error

SLC = Soil/Land use class

T = Temperature

WT = Water Table

Figures

Tables

Table of Contents

1. INTRODUCTION

Anthropogenically induced climate change will alter the hydrological cycle in the 21st century in the Nordic region, affecting the water balance and hydrological regime (IPCC 2013; Wada et al. 2016). In the long-term future, the Nordic region will likely experience substantial increase in temperature, and winter temperatures are expected to increase relatively more than summer temperatures. Precipitation will likely increase during winter and decrease during summer, and these trends have already been observed (Collins et al. 2013). Greenhouse gas emissions play an intrinsic role to the degree of change in water balance and hydrological regime (Maurer 2007). Depending on emission rate and concentration, the effects of climate change on all aspects will differ both in magnitude and timing due to the complexity of the climate system (Stocker et al. 2013). Climate change impact studies should therefore involve looking at different possible emission scenarios (Shrestha et al. 2016).

Assessing climate change impact on hydrology is an important motivation factor for future environmental monitoring programs (Lindström et al. 2010), research directions and for realising the Swedish National Environmental Objectives (Munthe et al. 2014). In Sweden, ecosystem research takes place on many different locations and in different environments. One such site is the Skogaryd research catchment; a nationally coordinated research site hosting studies on the interaction between terrestrial and limnological systems, as well as interfaces with the atmosphere[1]. Skogaryd research catchment consists of six sub-catchments of different characteristics, including a mire sub-catchment and a forest sub-catchment, hosting different soil matrix and land use, and where hydrological monitoring has been taking place since 2012. The site was officially established as a research site in 2013.

Characterization of catchment flow is important for research regarding water balance and water quality as a response to climate change, where models are vital tools (Xu et al. 2005). However, delineating differences in response between catchments of different characteristics currently poses great challenge for hydrological models (Clark et al. 2011). Since hydrological model input data, such as topography, soil property and vegetation, typically show large spatial heterogeneity there is a current demand for models that operate on sub-catchment scale (Lindström et al. 2010; Wada et al. 2016; McGlynn et al. 2003), as this would facilitate environmental projections for the future. Modelling climate change impact on the hydrological regime at sub-catchment scale therefore needs further scientific attention (Pham et al. 2015).

For the Skogaryd research catchment, where the constituent sub-catchments have not been part of a hydrological modelling project, this would mean a better understanding of the characteristically different sub-catchments in relation to flow and water quality runoff measured at the catchment stream outlet. The hydrological model HYPE (HYdrological Predictions for the Environment) is an integrated hydrological and water quality model that can be calibrated for both small and larger catchments (Lindström et al. 2010). HYPE has been successfully calibrated for smaller catchments in Sweden (Pers et al. 2016). The HYPE

[1] www.fieldsites.se/en-GB/about-sites/field-research-stations/skogaryd-32652394

model could therefore possibly be used to target contribution of runoff and solutes to the constituent sub-catchments of the Skogaryd research catchment.

Small streams are the main carriers of nutrients, pollutants and other elements originating from the terrestrial landscape. The hydrological connectivity between the soil matrix and the stream has large implications for the transportation of solutes. The bulk of the Earth's terrestrial carbon is stored in the soil (Crowther et al. 2016). A collective term for dissolved aromatic and aliphatic organic compounds in streams is Dissolved Organic Carbon (DOC). DOC is mainly formed by incomplete decomposition of plant material and is exported with soil runoff (Hope et al. 1994).

Dissolved organic carbon is a natural component of the aquatic ecosystem and plays an important role in chemical and photochemical reactions in fresh water (Sucker and Krause 2010; Pagano et al. 2014). The principal components of DOC are pigmented biopolymers; humic and fulvic acids. DOC is negatively related to pH and could influence acid-sensitive biota in fresh water streams, especially in already high DOC waters (Laudon and Buffam 2008). Due to its colouring effect of the stream water, increased concentrations could lead to implications for light penetration and affect photosynthetic organisms. Humic and fulvic acids are strong complexing agents and can make bioavailable several particle-bound metals in the soil, and thus serve as transport vectors for metals and organic pollutants (Laudon et al. 2012). DOC export is coupled to both export and speciation of metals, e.g. both quantity and the portioning between dissolved and particulate of Aluminium (Al) and Iron (Fe) can be coupled to DOC concentrations (Sucker and Krause 2010; Soto-Varela et al. 2014).

Concentrations of DOC have in general increased in European waters during the last decades and have scientifically been attributed to a warmer climate but also to recovery from acidification (Laudon and Buffam 2008; Sucker and Krause 2010). However, the production and transport of DOC from the terrestrial environment is not yet fully scientifically understood (Sucker and Krause 2010; Winterdahl et al. 2016). The trends and dynamics of redistribution of DOC from the terrestrial environment to downstream aquatic ecosystems are therefore central factors for determining the overall response to climate change of aquatic ecosystems and processes. Unveiling the controls of DOC intra-annual variability could thus provide a basis for evaluating long-term feedbacks of climate change (Winterdahl et al. 2014b; Winterdahl et al. 2016).

1.1 Aim of thesis

This project aims to 1) model and compare the water balance of two characteristically different sub-catchments; a forest on mineral soil-, and a mire in the Skogaryd Research catchment, by means of the hydrological model HYPE, 2) investigate the impact of climate change on the water balance, especially discharge, and 3) quantify DOC export by studying the control on the temporal DOC aquatic-terrestrial connectivity in the two sub-catchments. The following research questions guide the study:

1. Is HYPE applicable for modelling the hydrological regime from both sub-catchments in terms of quantity and dynamics?
2. How will climate change affect future water balance, and what is the difference between climate scenarios?
3. What is the controlling factor for DOC concentrations for both sub-catchments, and would it be possible to quantify long-term concentrations and mass flux?

This will be done by applying HYPE 4.13.2 (Lindström et al. 2010) to a mire and a forest catchment. DOC measured at the study site will thereafter be linked to other measured known physical controls and further linked to the previously modelled hydrological regime. Aims 2 and 3 will be carried out by comparing two 30-year periods, the climatological reference period of 1961-1990 (P1) and the long-term future (2071-2100) (P2) following different climate scenarios. The general methodology used in this study is presented in Figure 1.

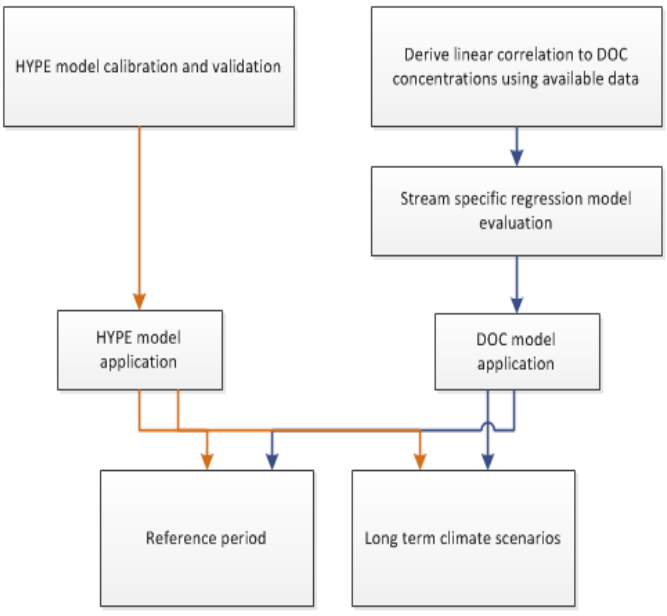

Figure 1. Flow chart of methodology used in this study to apply the hydrological model HYPE and quantifying discharge dynamics, water balance and DOC export. Red arrows refer to water fluxes and blue to DOC fluxes.

2. THEORETICAL BACKGROUND

2.1 Hydrological modelling

The main processes in a hydrological model are evapotranspiration, infiltration and percolation, soil moisture, snow accumulation and snowmelt, groundwater, above and below ground runoff processes, and eventually discharge at the catchment outlet. There is a vast number of hydrological models with a wide range of conceptualisation and representation which aim at not just modelling discharge at the outlet, but also the hydrological response to e.g. climate change, land cover and land use change (Koch et al. 2016). There are deterministic and stochastic hydrological models, where deterministic models try to represent empirical physical processes and are also the most commonly used (Efstratiadis et al. 2015).

During the last decades, hydrological models have been refined and improved to include more and further detailed aspects of the hydrological cycle (Strömqvist et al. 2012; Voeckler et al. 2014). Due to fact that it is difficult both to measure and empirically represent the vast spatial heterogeneity in natural systems, current understanding of mechanisms and dynamics at catchment scale is still incomplete. This has resulted in a large abundance of hydrological models (Clark et al. 2011). In general, with increasing complexity of the catchment there is also a higher discrepancy between different model results - where the model user also plays an intrinsic part of modelling results (Koch et al. 2016). The most common way to evaluate the model is to assess the "model fit" quantitatively, i.e. how well model results fit to observation data. When predicting response in discharge and water balance for a climate scenario, modelled climate data are used as input to the hydrological model. However, hydrological models calibrated for current conditions produce very different results for future scenarios (Jiang et al. 2007).

For a regional equivalence, downscaled climate data from Global climate models (GCM) can be used to simulate regional and local hydrological regime as a response to climate change (Reshmidevi et al. 2017). Much challenge of hydrological modelling at catchment scale in response to future climatic drivers of unknown temporal and spatial magnitude lies in that the models have been fitted to observed data or to fit past conditions and trends along a known temporal scale (Efstratiadis et al. 2015). The choice of hydrological model could therefore mean more to uncertainty than the global climate model used (Hagemann et al. 2012).

2.2 Climate change and its impact on hydrological regime in mire and forest catchments in the hemi-boreal region

2.2.1 Climate change and the hydrological cycle

Atmospheric concentrations of carbon dioxide (CO_2) have increased by more than 40% since 1750, along with increases of other greenhouse gases (GHG) (Hartmann et al. 2013; Chen et al. 2015). Consequently, global mean surface temperature has increased since the late 19th century and the first decade in the 21st century has been the warmest ever recorded. Since 1880, the global mean annual temperature (MAT) has increased with 0.85 $^{\circ}$C (Hartmann et al.

2013). If emissions of GHG continue unabated, further increases in MAT and an altered hydrological cycle are to be expected, especially on Northern latitudes (Hartmann et al. 2013).

On a global scale, there is a large natural variation in water flow and storage. Terrestrial water appears as surface water, such as river and lakes, soil moisture, groundwater, snow, ice and glaciers on the surface and permafrost. In the Nordic regions, increasing temperatures will decrease ice cover and snowpack. Increasing temperatures accelerate surface evaporation and plant transpiration, known as evapotranspiration (ET) (Stocker et al. 2013). Also, the amount of water that could go into evapotranspiration, potential ET (PET), will increase. Water vapour in the atmosphere will increase in a warmer climate since warm air holds more moisture, which can alter precipitation events. It is expected that events of extreme precipitation will increase in the future (Hartmann et al. 2013; Stocker et al. 2013). As a matter of fact, such a trend has already been noted (Hartmann et al. 2013).

Even if GHG emissions decrease substantially, it is beyond doubt that climate change will have a considerable impact on the Earth (Collins et al. 2013). The Intergovernmental Panel on Climate Change (IPCC) has outlined the response to climate change using different climate scenarios, i.e. the amount of energy that global warming will add to the climate system. The scenarios are so called Representative Concentration Pathways (RCP), which in words represent increased forcing in effective solar radiation (W m^{-2}) due to varying degrees of increases in GHG since pre-industrial levels. The scenarios used by the IPCC are called RCP2.6, RCP4.5, RCP6.0 and RCP8.5, where the number represents the respective increase by year 2100 in global radiation in W m^{-2}.

2.2.2 Hydrology and impacts of mire and forest catchments

Mires consist of peat soil which has been formed during slow decomposition under water-saturated conditions, and mires can therefore be characterised by all-year-round high water table (WT) (Mezbahuddin et al. 2016). They are usually covered by mosses (*Sphagnum* sp). Mires are either fens or bogs, where fens get their water from the surroundings, precipitation is the only water source for bogs (Grip and Rodhe 1994). The physical properties of the peat soil vary with depth, i.e. with increasing rates of humification. When the WT is high, mires have a fast response time to precipitation and water supply (Grip and Rodhe 1994; Laudon et al. 2007). Water travels near the surface or through the relatively large abundance of macro pores in the porous soil (Laudon et al. 2007). The water storage capacity is high due to high porosity. Due to the high-water content, mires freeze during cold periods, inhibiting infiltration – increasing the impact of overland flow contribution to discharge.

Under any climate scenario, the mire WT in Northern latitudes will likely decrease, however with a pronounced difference between fens and bogs, as fens receive their water from surrounding land, where recharge flows might attenuate (Grip and Rodhe 1994; Gong et al. 2012). This would also decrease discharge from mires, as the hydraulic conductivity is lower in deeper peat (Grip and Rodhe 1994; Gong et al. 2012), and further because the soils' water retention capacity increases, which will reduce peak flow and increase stream lag time (Holden 2005). A lower WT can also increase macro pore development leading to soil pipes. This, in turn, decreases the lag time, especially at extreme events (Holden and Burt 2002).

Mires play a majoring role in moderating global climate as they absorb CO_2 from the atmosphere (Grip and Rodhe 1994; Holden 2005). Mires store roughly 30 % of terrestrial carbon and cover approximately 2-3% of the Earth's total land mass (Freeman et al. 2012). The hydrological regime governs carbon storage and mass flux; hence, changes in the water balance on this relatively small scale can have large implications for global net carbon sequestration (Holden 2005). If the WT decreases, more oxygen gets in contact with peat soil and mineralisation rate of carbon and nutrients increases (Lyon et al. 2012).

Boreal and hemi-boreal forests in Sweden consist of mostly Norway spruce (*Picea abies)* and Scots pine (*Pinus sylvestris*). The canopy cover intercepts precipitation and thus governs the amount of precipitation that reaches the forest floor. The topography in a forest catchment often varies, which influences groundwater recharge and discharge (Grip and Rodhe 1994). The soil is usually coarse and the soil layer is thin. As for mires, the hydraulic conductivity increases near the surface such that a higher WT will lead to increasing discharge rate (Grip and Rodhe 1994). Most snowmelt water in a typical Swedish forest infiltrates in soils and small amounts of water go to surface runoff (Laudon et al. 2007). This gives the forest landscape a slower response time to precipitation compared to the mire. Soil frost does not substantially influence the infiltration capacity, however if the ground is frozen, higher peak discharge can be observed during snowmelt periods.

Climate change will lead to a prolonged growing season and could substantially increase in forest carbon sequestration, which could lead to a decreasing WT during growing season as transpiration is the most dominant process (Amatya et al. 2016). In addition, this could lead to decreasing discharge from forest catchments (Amatya et al. 2016). Snow melt-governed discharge will also decrease due to increasing soil and air temperatures substantially decreasing the snow pack.

2.3 Temporal and spatial dependence of DOC in hemi-boreal streams

DOC particles are in the size range from 10^{-10} to 10^{-6} metres and have a molecular weight of 10^{1} to 10^{8} (Laudon and Buffam 2008). In broad terms, DOC consists of non-humic fractions and humic fractions, further divided into humic acid, fluvic acid and humin. This report will however not discuss DOC composition further in detail. Microbial activity in the soil contribute to the humic fraction during humification of plant material. DOC gets suspended in the soil solution and is either microbially mineralized, adsorbed to soil particles or leached. Leaching of degraded organic material to the stream is one of the main sources of allochtonous DOC (Pagano et al. 2014). Also, the breakdown of microbial biomass itself is a source of DOC.

On a spatial scale, variations in DOC concentrations have been attributed to land cover, catchment size and pH (Ågren et al. 2007; Ågren et al. 2008; Winterdahl et al. 2014b; Wallin et al. 2015; Winterdahl et al. 2016). The composition and concentration of DOC in the water recipient largely depend on the external source, i.e. the characteristics of the soil matrix (Ågren et al. 2008; Weyhenmeyer et al. 2012; Olefeldt et al. 2013). The mobility dynamics of DOC is governed by soil pH, where more DOC gets mobilised at increasing pH

levels (Tipping & Woof 1990). Experiments using increasing pH in soils also showed increased enzyme activity, leading to enhanced DOC mobilisation (Pind et al. 1994).

The main identified drivers affecting DOC concentrations in streams on a short-term temporal scale are discharge and temperature, either in combination or as single variable controls – including variables such as soil moisture, soil frost, drought-induced acidification and winter length and severity (Soto-Varela et al. 2014; Winterdahl et al. 2014b; Wallin et al. 2015). On a temporal scale, variations in the DOC concentration of stream water are closely linked to air temperature and hydrological alterations (Hope et al. 1994; Hruska et al. 2009; Winterdahl et al. 2014b; Wallin et al. 2015; Weyhenmeyer et al. 2016).

Forests and mires have different temporal release patterns of DOC (Kokorite et al. 2010; Wallin et al. 2015; Kasurinen et al. 2016). Microbial and enzyme activity are related to temperature, where nutrient availability is a prerequisite for microbial activity. Experiments in peat soil have shown a strong correlation to DOC production under enhanced temperatures due to increasing microbial activity and especially enzyme activities that act like catalysing agents (Kane et al. 2014). Mires constitute an important source of freshwater DOC. The fraction of wetland coverage principally regulates DOC concentrations in adjacent streams; catchments of >40% wetland cover have significantly higher DOC loads than forested areas (Ågren et al. 2008).

Hydrology governs transportation of DOC, affecting the quantity and quality that reaches the stream (Pagano et al. 2014). In peat land-dominated areas DOC has shown strong temperature dependency and weak hydrological control, which has been explained by the homogenous soil profile with small or no differences in DOC concentrations along a vertical profile (Winterdahl et al. 2011; Winterdahl et al. 2014b; Wallin et al. 2015). This means that the groundwater table in mires has limited control on DOC as the peat soil is saturated all year around. High flush events therefore usually cause a decrease in DOC due to over land flow (Laudon et al. 2011). If the water table in peat soil is below the surface, full decomposition of soil organic matter take place which would decrease DOC concentrations in the soil layer. But a lower water table would also produce DOC that is available for release given a hydrological connectivity to the stream (Porcal et al 2009). A high precipitation event could there lead to a DOC flush event (Porcal et al 2009).

Dissolved organic carbon also originates from organic podzol soil profiles found in coniferous forest stands and from the upper organic soil layers in the riparian zone (Ågren et al. 2008). Spruce and pine species produce more DOC than do catchments covered by hardwood species (Kalbitz et al. 2000). DOC concentrations usually decreases vertically with depth in the podzol soil profile and therefore, the contribution of DOC from forest stands has been identified to be controlled by hydrological events, such as discharge, runoff and snow melt when the top soil layer is hydrologically connected to the stream. High flow events normally contribute to higher loads of DOC in adjacent streams (Ågren et al. 2008). In the mineral soil profile, DOC can be adsorbed to oxides and clay minerals, resulting in low DOC concentrations (Kalbitz et al. 1999).

3. MATERIALS AND METHODS

3.1 Site description

The studied sub-catchments are located within the Skogaryd Research Catchment (SRC; 58º23'N, 12º09'E, 75 m a.s.l., hemiboreal) in Västra Götaland, Sweden. Skogaryd Research catchment is part of the Swedish Infrastructure for Ecosystem Science, SITES; a nationally co-ordinated infrastructure for terrestrial and limnological field research[2]. The study areas were two characteristically different sub-catchments: a mire dominated catchment (MC) and a catchment with mineral soil covered by coniferous forest (FC) (Figure 2).

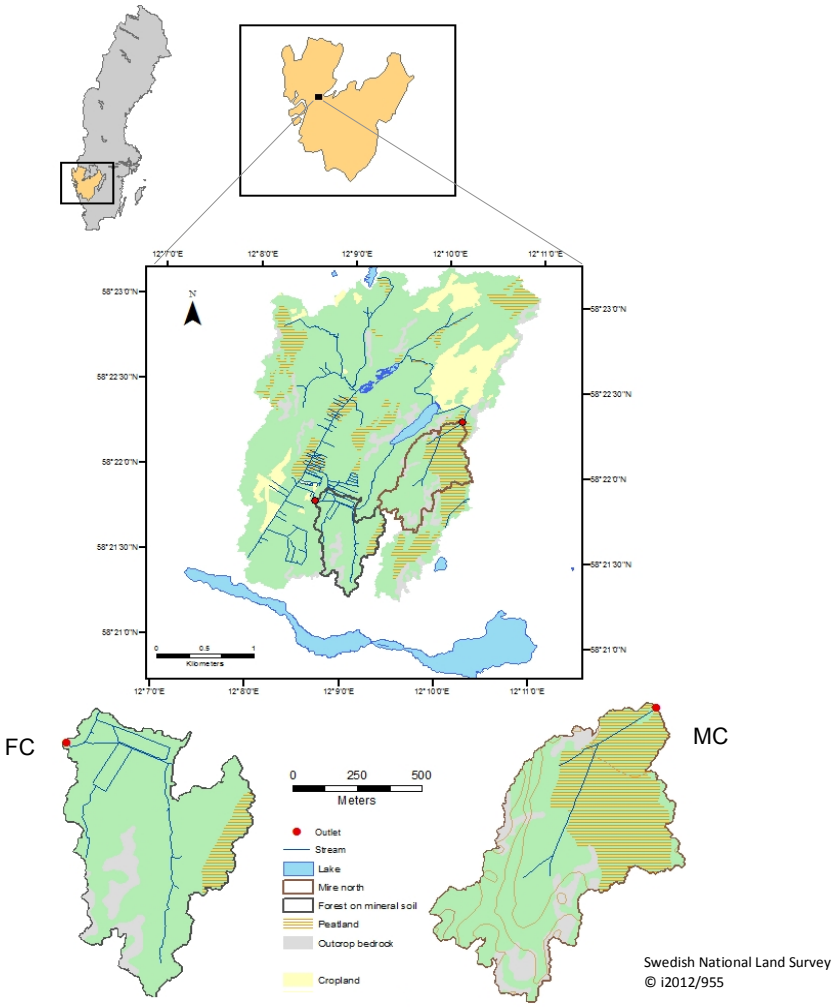

Figure 2. Location of Skogaryd Research Catchment (black box) and the two hemiboreal catchments, the forest on mineral soil and the mire. Skogaryd is located in Västra Götaland county, presented in yellow. Land use distributions are based on the topographic map (1:50.000) from Swedish National Survey.

[2] www.fieldsites.se/en-GB

Skogaryd Research Catchment (Figure 2). Norway spruce (*Picea abies)* and Scots pine (*Pinus sylvestris*) constitute the main tree species of both catchments (Meyer et al. 2013). Figure 3 shows the outlet at respective catchment.

Figure 3. Outlet and sampling point for the a) mire catchment at low discharge and b) forest catchment and peak discharge. Photo: David Allbrand.

The MC consists of an open minerotrophic fen (~40%) (Pers. communication, Leif Klemendtsson, 01-02-2017), mainly covered by mosses (*Sphagnum* sp), located near the catchment outlet, and mixed coniferous forest (age unknown) further up in the catchment, with a total area of 57 ha. The soils (> 0.5m depth) in general consist of peat (< 6 m thick) and granite bedrock, with elements of glacial clay (Figure 4). The FC has an area of 48 ha, covered by mixed coniferous forest (>90%). Approximately half of the FC consists of a first-generation coniferous forest grown on previous agricultural land located near the catchment outlet; the area was afforested in 1951. The other half consists of older forest of unknown age. The first stand of forest grows on a mix of glacial fine clay and post glacial fine sand and is classified as an umbrisol. Most of the ditches were carried out in the late 19th century to improve production as the area is a former agricultural land.

An acidic granite bedrock underline both FC and MC. The soil layer depth in both catchments varies between 0 and 10 m, with the deepest soil layers found in the northern parts of both catchments[3].

Temperature was measured at 10 km east of Skogaryd Research Catchment at Värnersborg SMHI monitoring station (58º36'N, 12º36'E). Long term mean annual temperature (MAT) (1961-1990) was 6.4 $^{\circ}$C (SMHI). Skogaryd is situated along a precipitation gradient with a west-east direction between two SMHI monitoring stations, Värnersborg and Uddevalla (58º37'N, 11º94'E). Precipitation for Skogaryd was calculated as a mean of the two stations, per methodology used by Meyer et al. (2013). The long-term (1961-1990) mean annual precipitation (MAP) was 765 mm.

[3] Soil layer © Geological Survey of Sweden (data collection 03-03-2017).

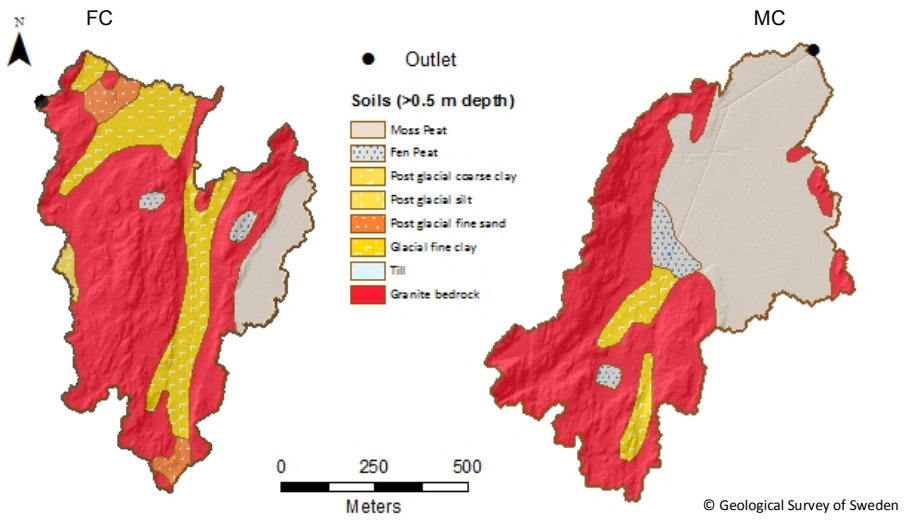

Figure 4. Soil layers (> 5 m depth) of the two hemiboreal catchments. Main stream outlet and sampling point is indicated by a black point for respective catchment. Soil layer © Geological Survey of Sweden

The two catchments were delineated using a high-resolution (2x2 m) digital elevation model (DEM). The hydrology toolbox in ArcGIS 10.0 (Environmental Systems Research Institute, Redlands, USA) was used to determine flow direction into each grid cell (2x2m), flow accumulation and catchment boundaries. A digital version of the topographic map (1:50000) provided information about the land use distribution. The DEM and the topographic map were provided by Swedish National Land Survey (© i2012/955). Information about soil conditions were based on the soil map (1:25000 – 1:100000) and a soil depth layer (10 x10 m), provided by the Geological Survey of Sweden. A field visit took place on the 19th of February 2017.

3.2 Model description

The model used in the study was HYdrological Predictions for the Environment (HYPE), version 4.13.2[4]. HYPE was identified as being suitable based on the purpose of the study and data availability. The model criteria of selection were: 1) daily temporal resolution, 2) should include equations for the most important processes governing water balance, and 3) should be able to apply on small catchments (Pham et al. 2015).

HYPE is a semi-distributed, deterministic, dynamic hydrology and water quality model that can be used for hydrological modelling on a small catchment scale (Hankin et al. 2016; Pers et al. 2016). It has been developed by SMHI and is provided as an open-source code model[5]. It has been used for i.e. hydrological forecasts and climate scenarios for basins in Sweden and elsewhere (Lindström et al. 2010; Strömqvist et al. 2012; Donnelly et al. 2014; Pechlivanidis et al. 2015; Pers et al. 2016). The model is a continuous process based model

[4] www.hypecode.smhi.se
[5] www.hypecode.smhi.se

that applies a multi-basin approach, and is thus suitable for basin modelling also on a large scale.

HYPE simulates components of the catchment water cycle at a daily time step and allows for detailed description of the topography, land use and soil class of each sub-catchment. The accumulated flow is directed to streams and lakes that can be specified within each sub-catchment and conceptually routed between sub-catchments within a catchment (Hankin et al. 2016; Hundecha et al. 2016). The major land and subsurface processes included are surface runoff, groundwater outflow from soil, snow accumulation and snowmelt, macro pore flow and evapotranspiration (Lindström et al. 2010; Donnelly et al. 2014; Pers et al. 2016). Hence, the main sources and sinks of water flow are included. HYPE also contain equations for modelling nutrient (Nitrogen, Phosphorous, Carbon) deposition, transport and turnover (Pers et al. 2016), however, those were not applied in this study due to lack of essential observation data.

The HYPE model sub-divides the catchment into different discrete Soil and Land Use Classes (SLC), which are the smallest computational spatial units (Hankin et al. 2016). Each SLC is based on a combination of soil type and land use, further specified between one to three soil layers of different depth and characteristics. The SLCs are defined as a fraction of a sub-catchment area, and are hence not coupled to a geographical location (Lindström et al. 2010). Lakes constitute their own SLC class. Every SLC class has its own 'vertical schematization' for estimation of water balance. Parameter set up is based on desired output and level of detail. Some parameters are directly linked to soil type or land use/crops, whereas others are global in that they are linked to the entire model domain (Strömqvist et al. 2012). For instance, water holding capacities are linked to soil type, whereas threshold parameter for snowmelt is assigned to land use type, see Appendix I for details.

HYPE performance criteria can be computed by the model. The model has no graphical user interface, as both input and output data are provided as text files. The input and result data can be viewed and analysed in e.g. a geographical information system (GIS). In this study, model results were processed in Excel.

3.2.1 Processes in HYPE

There are several flow paths for precipitation in the soil (Figure 5). A set threshold value (*ttmp*) for air temperature partitions precipitation as either rain or snow, or a mixture of the two. Water flow from snow melt is simulated using the degree-day method; for each degree Celsius above an average of 0 °C, a certain mm d^{-1} of snowmelt is produced depending on the locations' exposure to wind and solar radiation (Lindström et al. 2010). Parameter values used in this study are presented in Appendix I. Equations are due to copyrights not printed but can be found in Lindström et al (2010).

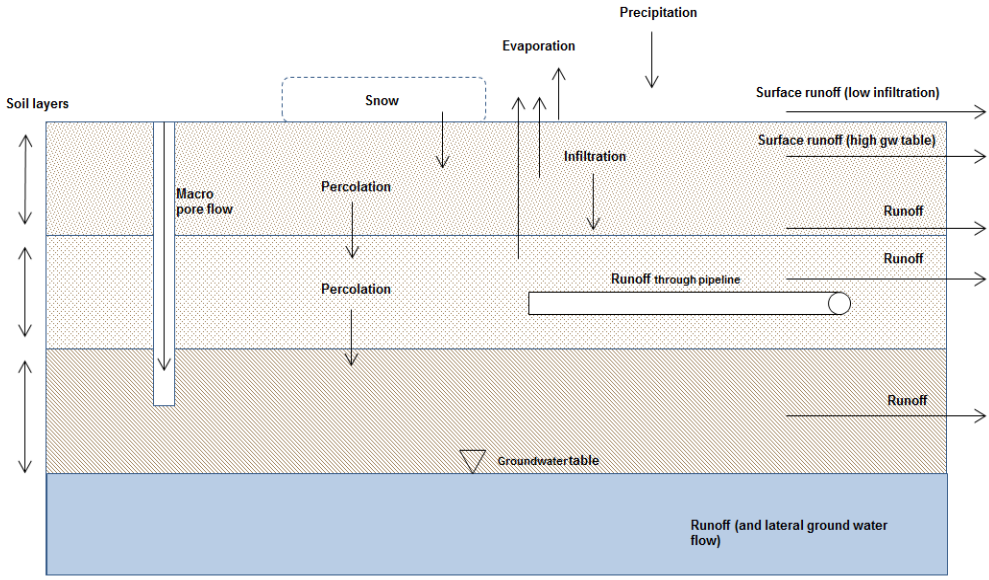

Figure 5. Illustration of possible flow paths in the soil in the HYPE model. Modified from Strömqvist et al (2012).

Potential evapotranspiration (PET) is calculated based on air temperature and is assumed to occur when air temperature is greater than *ttmp* (threshold temperature) and if soil water content exceeds a large proportion, *lp*, of the soil field capacity (*wcfc*). The threshold temperature is used to drive both snowmelt and evaporation. PET is also dependent on the rate parameter for PET (*cevp*). A seasonal factor (*cevpcorr*) adjusts PET by making it higher in spring and lower in autumn. Potential evapotranspiration only occurs from the two upper soil layers, and is assumed to decrease exponentially with soil depth (Lindström et al. 2010; Hundecha et al. 2016). Below the field capacity (*wcfc*, mm) and wilting point (*wcwp*, mm), actual evapotranspiration decreases linearly, while ET = PET if soil water exceeds *wcfc* or a large portion of *wcfc* (*lp*, mm).

In HYPE, water infiltrates through the soil pores. Water percolates down from an upper to a lower soil level when the field capacity is exceeded, using a percolation parameter (*mprec*) (Hundecha et al. 2016). Surface runoff and macro pore flow occurs if given parameter threshold values for maximum infiltration rate for the soil class (*mactrinf*), and threshold soil water for macro-pore flow and surface runoff (*mactrsm*), are both exceeded (Hundecha et al. 2016). This type of macro pore or preferential flow is called double hump. It describes preferential flow (near-) saturation, but is known to underestimate sharp increases in peak flow and thereby the highest peaks as well as excluding preferential flow under dry conditions, for instance in cracks (Gärdenas et al. 2006). Marco pore flow is directed to the groundwater table (GWT). Groundwater is simulated by the water content of the soil, and is calculated based on the proportion of water-filled pores of effective porosity. When the largest pores begin to fill, groundwater outflow takes place from the soil layer beneath (Strömqvist et al. 2012).

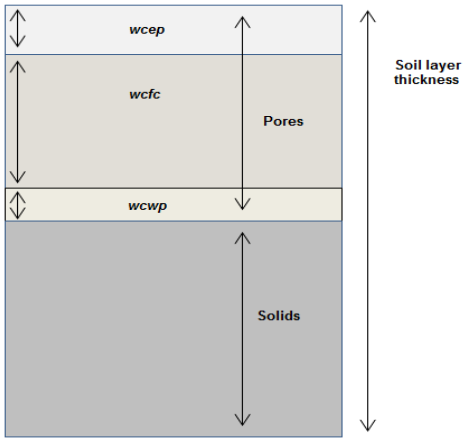

Figure 6. Water retention parameters found in HYPE 4.13.2. Modified from Lindström et al (2010).

Soil wetness is in the model derived from water balance computations for each soil layer. Three fractions govern soil water storage (Figure 6). The first parameter, wilting point (*wcwp*) sets the fraction that cannot be evaporated. The second parameter, field capacity (*wcfc*), sets the water fraction that can be evaporated but that cannot be emitted as discharge, which is the soil field capacity. The third parameter, effective porosity (*wcep*), sets the fraction that can be emitted as evaporation or runoff. The sum of these three fractions corresponds to the total possible water content of the soil (Lindström et al. 2010; Strömqvist et al. 2012). Both soil type and soil layer influence the possible water content in the HYPE model.

Groundwater runoff can occur from all soil layers, and depends on the water table level in relation to the drainage depth and on water content in the effective porosity. This occurs when soil moisture content reaches above field capacity, using a soil type dependent recession coefficient (*rrcs*). Runoff takes place down to the drainage depth, i.e. in the case the stream drainage level is in the second soil layer and that soil layer is not saturated, runoff is dependent on the water level above the drainage level (Lindström et al. 2010; Pers et al. 2016). Soil layers located below drainage depth have no groundwater runoff.

3.3 Model input data

3.3.1 Field sampling

Discharge measurements were made at both sub-catchments outlets by SITES Skogaryd using installed fumes, where stage height was recorded by an ultrasound sensor (710, MJK Automation, Sweden), every 10 minutes for the years 2012-2013 and every 15 minutes for the years 2014-2016, both connected to the ISCO station (2110, Teledyne ISCO, USA) (Table 1). Mean daily discharge (Q) was derived from shaped stage-height-discharge rating curves ($R^2 >$ 0.9) from a site specific V-shaped notch (90° angle). The rating curves were verified by a series of manual discharge measurements using a handheld Flow Tracker device (SonTek, San Diego, USA). Specific discharge (q) was calculated by normalizing Q to the sub-catchment area to provide a basis for between sub-catchment comparisons.

The two streams were manually sampled every two weeks April to December 2012-2016 using high-density polyethylene bottles of 250 ml for analysis of DOC. Samples were collected without headspace and were kept dark and cold during transport to the laboratory. In total, 77 and 64 samples of DOC concentrations (also denoted [DOC]) were used in the analysis for the mire and forest catchment, respectively. When the streams were dry, such as during late summer and early autumn of 2013, no samples were taken.

Local temperature data was measured with a Rotroninc HMP45C Temperature probe (Campbell Scientific Inc.) at an Eddy Covariance (EC) flux tower in mire catchment, 1.5 m above ground (Table 1). The sensor was mounted in a ventilated radiation protection. Data existed for the years 2013-2016.

Local precipitation data was measured at the mire catchment site, using a SBS500H Tipping bucket precipitation sensor (Campbell Scientific Inc.). The sensors were measured every 30 second and a mean value was calculated every 30-min using a Campbell Scientific CR1000 datalogger. Data existed for the years 2013-2016.

Table 1. Type, resolution and source for the data used in the study.

Data type	Data	Resolution	Source
Geographical data	GSD-Elevation data, Grid 2+	2x2 m	Swedish National Land Survey © i2012/955
	Soil type	Raster, based on sampling with varying spatial resolution	Geological Survey of Sweden
	Land use	Vector	Geological Survey of Sweden
	Soil depth	10x10 m	Geological Survey of Sweden
Meteorological data	Temperature	10 minutes	Campbell CS100 Barometric Pressure Sensor and SMHI (2017a)
	Precipitation	10 minutes	Campbell CR1000 datalogger and SMHI (2017b)
Climate projection data	Mean temperature	Daily	Tinghai Ou (Department of Earth Sciences, University of Gothenburg)
	Mean precipitation	Daily	Tinghai Ou (Department of Earth Sciences, University of Gothenburg)

3.3.2 Climate change projections

Statistically downscaled climate data for temperature and precipitation was used as climate projection data for the 21st century. Data was provided for three climate scenarios, RCP2.6, RCP4.5 and RCP8.5, interpolated from the CSIRO-Mk3.6.0 Atmosphere Ocean Global Climate Model (ACGCM) (Collier et al. 2011). The climatic model has a spatial resolution of approximately 1.9°x1.9° (Collier et al. 2011). Temperature and precipitation was modelled as

daily averages (1950-2100), with climate forcing relative to RCP2.6, RCP4.5 and RCP8.5, starting in 2006.

Inverse Distance Weighed Interpolation (IDWI) from four modelled (CSIRO-Mk3.6.0 ACGCM) grid values was used to derive a daily mean for a grid covering south of Sweden, SRC; 56º0'N, 13º5'E, approximately (Table 1). The data was chosen to represent local projections for the Skogaryd Research Catchment.

3.4 Model application

3.4.1 Regional bias correction

Statistical downscaling has demonstrated incapability of reproducing temporal and spatial variability (Milly and Eagleson 1988; Hwang and Graham 2014). Skogaryd daily observations of precipitation and temperature were therefore used to reproduce spatial auto-correlation to normalise the regional model bias. Average monthly values for 1961-1990 (P1) were compared to average monthly values of the climate data in P1. As the precipitation bias was not evenly distributed over the year, a monthly correction factor was calculated that corrected each RCP scenario in P2. On average, modelled precipitation values had a negative bias compared to observations of 93 mm y^{-1}. Similarly, modelled temperature had an average negative bias compared to observations of 1.53 $^{\circ}C$ y^{-1}. Temperature bias for P2 was corrected for by adding the average monthly discrepancy between modelled values and Skogaryd. Missing leap years were inserted in P2 and precipitation values of 29 February were put to 0. As for leap year temperature, the value was a mean of the proceeding and preceding value.

3.4.2 Soil and Land Use Classes

Soil and Land Use Classes (SLC) were derived by combining soil type and land use information from the Swedish Geological Survey in ArcGIS 10.2.2, resulting in several individual classes each containing one land use and one soil type. This was done subsequently after transforming all layers into raster with a 2-m spatial resolution to match the elevation files. The SLCs with areas below 20 m^2 were joined to the adjacent SLC. As a simplification, different types of clays where joined to form one clay soil type. Moss peat and fen peat (Figure 3) were joined into one peat soil type (Figure 7).

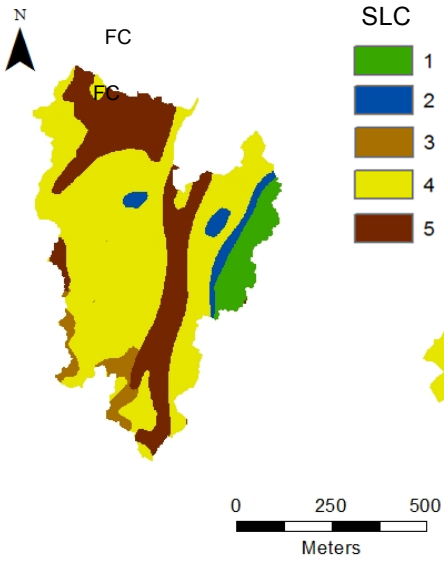

SLC	Land use	Soil type
1	Fen	Peat
2	Coniferous forest	Peat
3	Coniferous forest	Thin soil over bedrock
4	Coniferous forest	Coarse soil
5	Coniferous forest	Clay

Figure 7. Summary of land use and soil type (SLC) used in the model set up. The land use and soil type that constitute a SLC are presented in the table.

Orthophoto[6] and soil depth information were used for validation of the SLC classes. The SLC classes were also compared to predefined SLC classes of Swedish sub-catchment 4147 as modelled in S-HYPE (Strömqvist et al. 2012)[7] of which the Skogaryd Research Catchment is a part. For both catchments, the soil depth was zero or just above zero (Figure 4). However, the area was covered by sparse coniferous forest, suggesting that there was a soil layer covering the granite bedrock. To account for the heterogeneity in the relatively large part of the area with coniferous forest on granite bedrock the soil type was set to a porous thin soil, equivalent to a coarse soil type.

3.4.3 HYPE set-up

In this study the model time step was daily, and the model was only set to model hydrology. The input data used in the model set up was daily time series of discharge (*Q*obs), precipitation (*P*obs) and mean temperature (*T*obs) (2012-2016). The timescale of observed Q was changed into mean daily values (m^3 s^{-1}) to fit model requirements. The discharge data was manually scanned, and days with ≥ 50% missing values were assigned -9999. If the observed *Q*-value at a certain time step was zero or less than zero, the value was assigned -9999, as this was how the model handled missing values. Regarding temperature, days of which values were missing (<20 for the entire period), were filled with temperature data from

[6] GSD-Ortofoto, SWEREF99, © Swedish National Land Survey.
[7] www.vattenweb.smhi.se

Värnersborg SMHI monitoring station. Missing values in the *P*obs file were substituted with -9999. Precipitation for 2012 was replaced per methodology presented in section 3.1.

The year of 2012 was used as a model warming-up period (Lindström et al. 2010). The years 2013-2014 were used as model calibration years and 2015-2016 as model validation years. The number of decimals for the model output was put to 6, giving the lowest possible output a value of 0.000001 m^3 s^{-1}. The DEM was used to derive the average slope of each sub basin. Stream depth and number of soil layers were also defined and connected respective SLC. The two catchments were modelled during the same model run.

3.4.4 Performance criteria

The criteria used to evaluate model performance were Nash-Sutcliffe efficiency (NSE), Pearson's correlation coefficient (CC), relative bias (RB) and root mean square error (RMSE). Nash-Sutcliffe efficiency (Nash and Sutcliffe 1970) is a common coefficient of efficiency in hydrological modelling, and combines several aspects of the simulation (Moriasi et al. 2007). The NSE can vary between -∞ and 1. If the NSE value is 1, the model output is identical to measured/observed data. Values above 0.5 can be considered as satisfactory, and values above 0.7 as very good (Moriasi et al. 2007). In addition, RB was here used to assess the average value and CC to assess the timing of the discharge, accompanied by visual inspection of the entire time series. Calculations of NSE, CC, RB and RMSE are computed as per equations (1), (2), (3) and (4), respectively:

$$NSE = 1 - \frac{\sum_{i=1}^{m}(c-r)^2}{\sum_{i=1}^{m}(r-\bar{r})^2} \quad (1)$$

$$RB = \frac{\sum_{i=1}^{m}(c-r)}{\sum_{i=1}^{m} r} \cdot 100\% \quad (2)$$

$$CC = \frac{\sum_{i=1}^{m}(c-\bar{c})\cdot(r-\bar{r})}{\sqrt{\sum_{i=1}^{m}(c-\bar{c})^2 \cdot \sum_{i=1}^{m}(r-\bar{r})^2}} \quad (3)$$

$$RMSE = \sqrt{\overline{(c-r)^2}} \quad (4)$$

where c indicates a simulated value and r an observed value. $\bar{r}$ and $\bar{c}$ denote the mean over a period of m values.

3.4.5 Assumptions

Most of the participating model equations were connected to field capacity, wilting point and effective porosity. These parameters were given fixed values and were hence not included in the calibration. The values for *wcfc*, *wcwp* and *wcep* for each soil type except the clay soil, were acquired from the literature (Grip and Rodhe 1994; Ashman and Puri 2002; Parent and Illnicki 2003; Hartge and Horn 2016). Due to time limits, no field measurements of the literature derived values were conducted.

Mechanical analysis from three samples of mineral soil from different sites, performed in 2007, was used to derive *wcfc, wcwp, wcep* of the clay soil. First, three model simulations were performed with altering *wcfc, wcwp, wcep* values representing the conditions at the three different sites and where the other parameters were assessed from common intervals, which were given in a HYPE code demo file. The best simulation (NSE and CC) was then chosen to represent the entire clay soil.

The stream depth was set to 0.5 m in the peat soil and 0.6 m in the remaining areas (Pers. communication, David Allbrand, 20-03-2017). No drainage pipes were included in the model set up.

A vegetation steady state was assumed throughout the 21nd century as the HYPE model does not include dynamic vegetation. Further, it was assumed that water supply is entirely in the form of precipitation over the catchment area and that there was no lateral groundwater flow between catchments.

3.4.6 Model calibration and model validation

Prior to model calibration, included parameters were assigned values based on existing demo files in a trial and error approach to discern the model's sensitivity to altered parameter values and to explore the behavioural structure of the model. A limited literature review was also conducted to outline a calibration aim (Janssen and Heuberger 1995).

The calibration was done in two steps. First the weakest part in the agreement between observed and modelled discharge was identified. These were the peak flows. Consequently, parameters related to macro pore flow (*mactrinf, mactrsm, macrate*) were calibrated using by 1000 Monte Carlo simulations to find optimal values (Simunek et al. 2003; Gärdenas et al. 2006) (Table 2). As only three parameters were simulated, 1000 simulations were considered enough. Next, the remaining parameters that were not constant values were calibrated during a Monte Carlo simulation of 5000 runs (Table 3). Only global parameterisation was conducted, which means that all parameters were calibrated at the same time, as many processes are inter-connected and inter-dependent on each other (Ortiz et al. 2013). Hence, no individual parameterisation took place.

Table 2. Parameters that were calibrated in the first round using a Monte Carlo simulation of 1000 runs, including range used in calibration. The final parameter values are presented in Appendix I.

Parameter	Description	Unit	Min	Max
mactrinf	Threshold for macro pore flow	mm d^{-1}	5	50
mactrsm	Threshold soil water as a function of soil depth for macro pore flow and surface runoff	-	0	1
macrate	Fraction of macro pore flow	-	0	1

Table 3. Parameters that were calibrated in the second round using a Monte Carlo simulation of 5000 runs, including range used in calibration. The final parameter values are presented in Appendix I.

Parameter	Description	Unit	Min	Max
rrcs1	Soil runoff recession coefficient for uppermost soil layer	-	0.05	1
rrcs2	Soil runoff recession coefficient for lowest soil layer	-	0.0001	0.05
mperc1	Maximum percolation capacity from 1st to 2nd soil layer	mm d^{-1}	0.1	100
mperc2	Maximum percolation capacity from 2nd to 3rd soil layer	mm d^{-1}	0.1	100
srrate	Fraction of surface runoff	-	0.01	1
cmlt	Degree-day factor	mm d^{-1} $°C^{-1}$	1	5
cevp	Rate for basic potential evapotranspiration	mm d^{-1} $°C^{-1}$	0.05	0.7
ttmp	Threshold temperature for snowmelt	°C	0.1	0.5
frost	Frost depth parameter	cm $°C^{-1}$	0.5	0.5
srrcs	Recession coefficient for surface runoff	-	0.05	0.5
lp	Threshold soil water for activation of PET	%	0.7	1
rrcs3	Slope dependent recession coefficient in the upper soil layer	d^{-1}	0.0001	0.0003

The model calibration period was 01-06-2013 to 31-12-2014. Observed discharge in early 2013 contained a lot of missing values, and was therefore excluded from the calibration. HYPE 4.13.2 did not differentiate between base flow and peak flow; emphasis was therefore on getting a good fit of the base flow and smaller peaks as well as timing of discharge (Janssen and Heuberger 1995; Gärdenas et al. 2006).

The model calibration was evaluated based on overall efficiency (NSE), average value (RB), the timing of the discharge (CC) and average model performance (RMSE). Emphasis was put on obtaining a good value on NSE (Moriasi et al. 2007). As a complement to model performance measures, which are based on the complete time series, fitting to base flow and smaller peaks was also evaluated by visual inspection as yearly discharge has a large inter-annual fluctuation.

To provide a basis for discussion and a more thorough analysis of model performance, a sensitivity analysis was conducted by plotting each parameter to the corresponding NSE for

all 5000 Monte Carlo simulations. CC was also calculated for all parameters. These results are presented in Appendix II.

Model validation was done on the full years of 2015-2016 by applying the parameter set up used for the calibration. Seasonal validation was conducted to see how well the model performed for different seasons. 01-12-2015 to 28-02-2016 was chosen for winter validation, 01-03-2016 to 31-05-2016 as spring validation, 01-06-2016 to 31-08-2016 as summer validation and 01-09-2016 to 30-11-2016 as autumn validation.

3.5 Analysis and calculations

3.5.1 Discharge

As neither precipitation data nor discharge data was normally distributed (Shapiro-Wilk test), the non-parametric Spearman's rank correlation test (Spearman rho) was used to test correlations between explanatory variables and discharge, and correlations between the two catchments. Significant difference or correlation in timing and magnitude between the two catchments was tested with the nonparametric Wilcoxon's test. Correlations and differences between the catchments were considered significant if $\rho \leq 0.05$. IBM SPSS Statistics 20 was used for all statistical analysis.

3.5.2 Water balance

The water balance mass equation was used to calculate changes in the amount of precipitation that goes into discharge, evaporation and storage as per (5):

$$P = Q + E + \Delta S \tag{5}$$

where P is precipitation (mm), Q is discharge (mm) and ΔS is storage (mm). Storage was calculated by subtracting the total sum of discharge and evaporation from precipitation over the full 30y period. Numbers were rounded off to integers. Both Q and E were simulated by HYPE. Evaporation in the HYPE model (version 4.13.2) is calculated as described in Section 3.1.1.

3.5.3 DOC model development

DOC was not modelled in HYPE 4.13.2 due to lack of essential model input data. Measured DOC (mg L^{-1}) for the years 2012-2016 for the two streams was instead used to explore simple temporal relationships on DOC concentrations using available variables; 77 and 64 samples of DOC concentrations were used for the mire and forest catchment, respectively.

Automatic linear modelling (ALM) (regression analysis of the first order), with a 95% confidence level was used to explore drivers of temporal [DOC] variability, based on relationships between lateral export of DOC and a set of explanatory variables. ALM is a form of linear regression analysis that returns the explanation factor for each variable but also the joint explanation factor of all variables above the confidence level. It is therefore possible to see if several joint variables can predict DOC concentration. The method is limited in the

sense that it provides only first order regression equations for each used variable. ALM was chosen due to time and computing programme availability. The analysis was conducted for the full period only and not for individual years, hence only the seasonal dynamics was analysed.

The variables used in the ALM analysis have been identified as important drivers of DOC concentrations in streams from previous studies in the area and of catchments with similar characteristics (Dinsmore et al. 2013; Wallin et al. 2015; Winterdahl et al. 2016). The selection of variables was also based on data availability as no other data was available for analysis. The explanatory variables were temperature (T), and specific discharge (q) for the day of sampling as well as q measured 14 days prior to the sampling day (denoted q_{-14}). In addition, average values of T 30 and 60 days prior to the sampling day (denoted T_{avg30} and T_{avg60}) were used to investigate DOC connectivity between the terrestrial and aquatic environment in the ALM analysis. IBM SPSS Statistics (Version 20.0. Armonk, NY: IBM Corp.) was used for the statistical analysis.

The resulting best explanatory catchment-specific regression model was used to model export and concentrations of DOC for P1 and P2. The RMSE was calculated based on modelled and measured values at sampling date (2012-2016). Differences in DOC quantity between the two streams were tested by the nonparametric Wilcoxon's test. Correlations between explanatory variables and export of DOC were tested using the nonparametric Spearman's rank correlation test. Differences and correlations were considered significant at $p < 0.05$. Observed concentrations (mg L^{-1}) were used to validate the catchment-specific temperature-dependent regression model using a visual comparison to P1, as too few observed values existed to be used in any statistical analysis.

Export of DOC was calculated as the sum daily [DOC] multiplied by average daily discharge (Q). The specific export was obtained by normalising DOC export to the area of the catchment. By normalising the annual export to annual runoff, flow-weighted [DOC] could be calculated. Uncertainty was estimated using a standard deviation of 12%, which is in line with findings from studies using similar analytical and hydrological methods (Ågren et al. 2007; Nilsson et al. 2008; Wallin et al. 2015).

3.6 Discharge patterns

Observed discharge was ~440 mm y^{-1} for the MC and ~520 mm y^{-1} for the FC (dataset included missing values). Discharge distribution between the streams (2012-2016) was very similar ($\rho = 0.91$, $p \leq 0.0001$, $n = 1578$, Spearman rho). Specific discharge (q) for the MC was ranging from 0 to 26.83 mm d^{-1} (median 0.37 mm d^{-1}), whereas q for FC ranged from 0 to 24.35 mm d^{-1} (median 0.68 mm d^{-1}) during the 5-year period. Most high-discharge days for both streams occurred during autumn and early winter months. Mean annual temperature for 2012-2016 was 7.8 °C, which is 1.4 °C warmer than MAT during P1. Mean annual precipitation was 974 mm, which was 40% higher than MAP during P1. Temperature dependence on discharge was larger than the precipitation dependence (Table 4).

Table 4. Correlation coefficient (Spearman's rho) between specific observed discharge (q) and temperature (T), precipitation 1 day prior to discharge (denoted P_{-1}) and precipitation (P) (2012-2016). Correlations were significant at a 0.01 level. n = number.

	T (°C)	P_{-1} (mm d^{-1})	P (mm d^{-1})
	ρ (n)	ρ (n)	ρ (n)
MC	-0.45 (1780)	0.42 (1590)	0.34 (1591)
FC	-0.47 (1596)	0.44 (1404)	0.35 (1403)

3.7 Climate scenarios

Period 2 MAT was 9.1, 9.3 and 11.2 °C for RCP2.6, RCP4.5 and RCP8.5, respectively. Temperature is projected to increase with 2.7, 2.9 and 4.8 °C in period 2 (2071-2100), relative to P1 (6.4 °C). MAP for P2 was 820, 822 and 827 mm for RCP2.6, RCP4.5 and RCP8.5, respectively; a projected increase with 55, 57 and 62 mm relative to P1 (765 mm) (Figure 8a-b). The increase in temperature is largest during winter, early spring and summer. RCP2.6 and RCP4.5 showed more similar patterns of projected temperature and precipitation than RCP8.5.

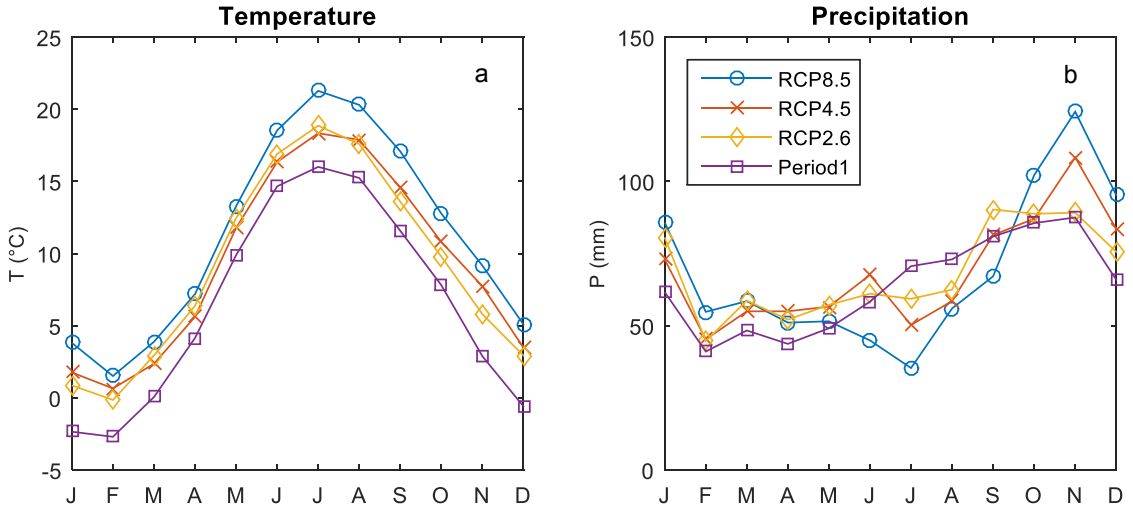

Figure 8. Average monthly a) temperature (°C) and b) precipitation (mm) for P1 and P2 (projected).

4. RESULTS

4.1 Model calibration and validation

Model performance for the calibration was very good (NSE=0.83 for both catchments) (Figure 9). There was a slight offset in the timing (CC) of modelled discharge compared to the observed in winter and early spring for both catchments. The RB indicated an underestimation of discharge for the MC and, on average, a slight overestimation of discharge for the FC. The RMSE indicated an overall very large agreement for the modelled values.

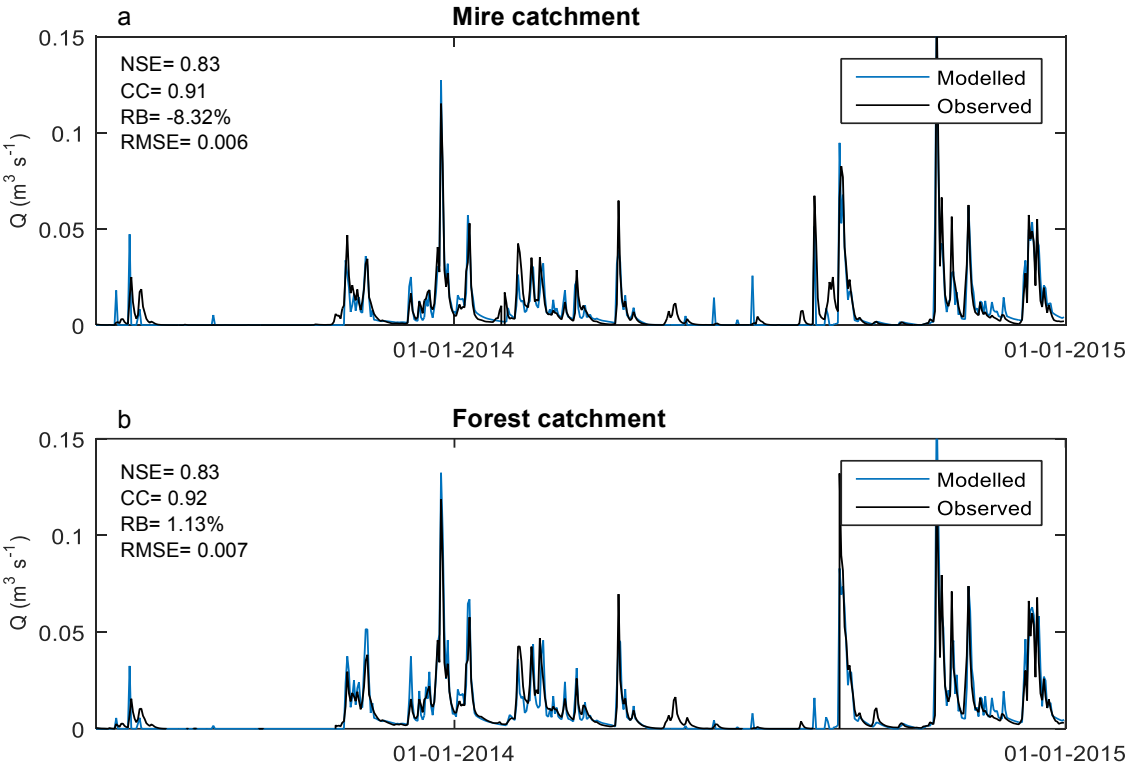

Figure 9. Calibration of HYPE for a) mire catchment and b) forest catchment. Calibration period with observations: 01-06-2013 to 31-12-2014.

Both peak and base flow were well captured, based on visual inspection; however, the model overestimated discharge for some peaks. The FC showed an overestimation of peak and base flow during winter 2013/2014. Summer discharge was particularly distinguished by the presence of uncorrelated peaks for both catchments.

Model performance for the validation period was also good, however NSE decreased with 0.09 and 0.08 for the MC and FC, respectively (Figure 10). There was a slight decrease in timing of modelled discharge (CC), and a large decrease in average value (RB), especially for the FC, which was most evident in spring and summer 2015. There were two observed peaks

in late spring 2015 which were not captured at all by the model due to missing observed precipitation data. The overall fit (RMSE) lowered slightly compared to the calibration.

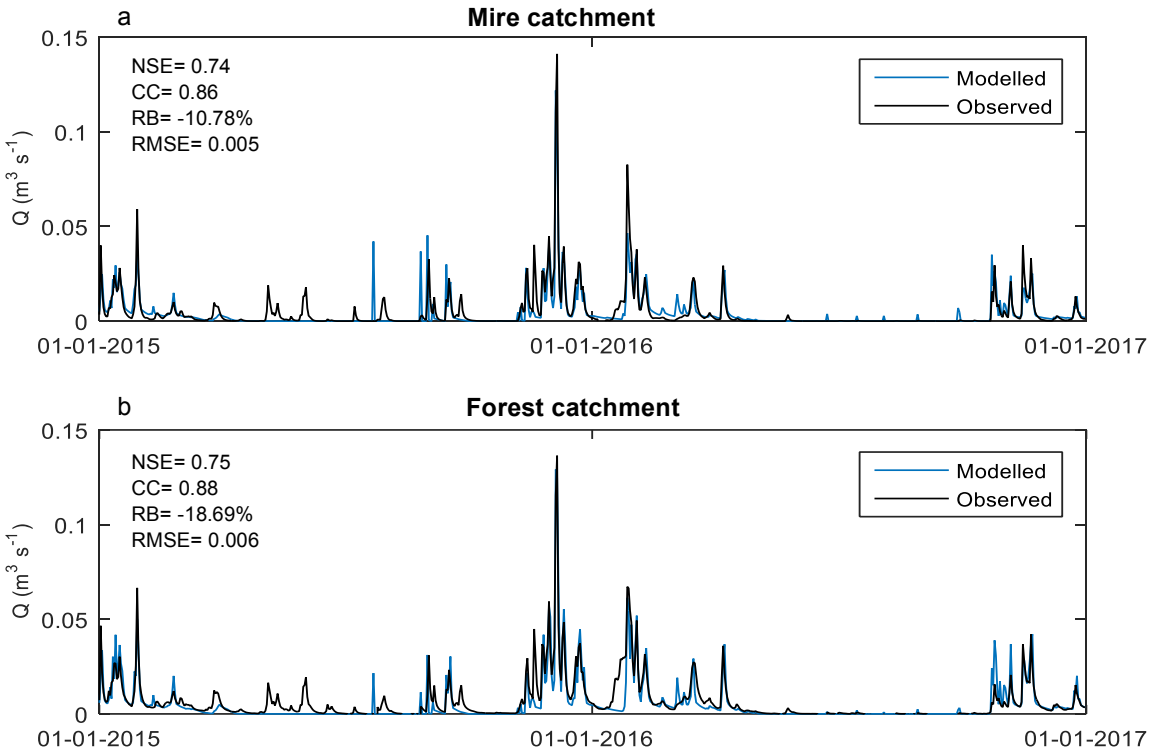

Figure 10. Validation of HYPE of a) mire catchment and b) forest catchment. Validation period with observations: 01-01-2015 to 12-31-2016.

There was a large discrepancy in model performance between seasons (Figure 11); however, orders of magnitude for all four seasons coincided for the two catchments. The MC had a summer (Jun, Jul, Aug) NSE of -270.44, compared to validation period NSE of 0.74. Modelled summer discharge was at places 10 times the observed discharge (Figure 11e). The FC had a summer NSE of -2.8, compared to the whole period validation with NSE=0.75 (Figure 11f). In general, the model captured the other seasons well or very well, based on threshold limits for NSE from Moriasi et al. (2007). The best fit occurred during the winter season (Dec, Jan, Feb), where both peaks and base flow were well captured by the model, except for one week during late January due to missing precipitation data (Figure 11a-b).

The spring flood was well captured by the model, however in early March there was a modelled peak that did not coincide with observed discharge (Figure 11c-d). The model simulated autumn discharge very well for the MC, however the performance was bad for the FC, mostly due to a simulated discharge in November not coinciding with observed discharge. Winter and spring peaks were in general better captured by the model than autumn peaks.

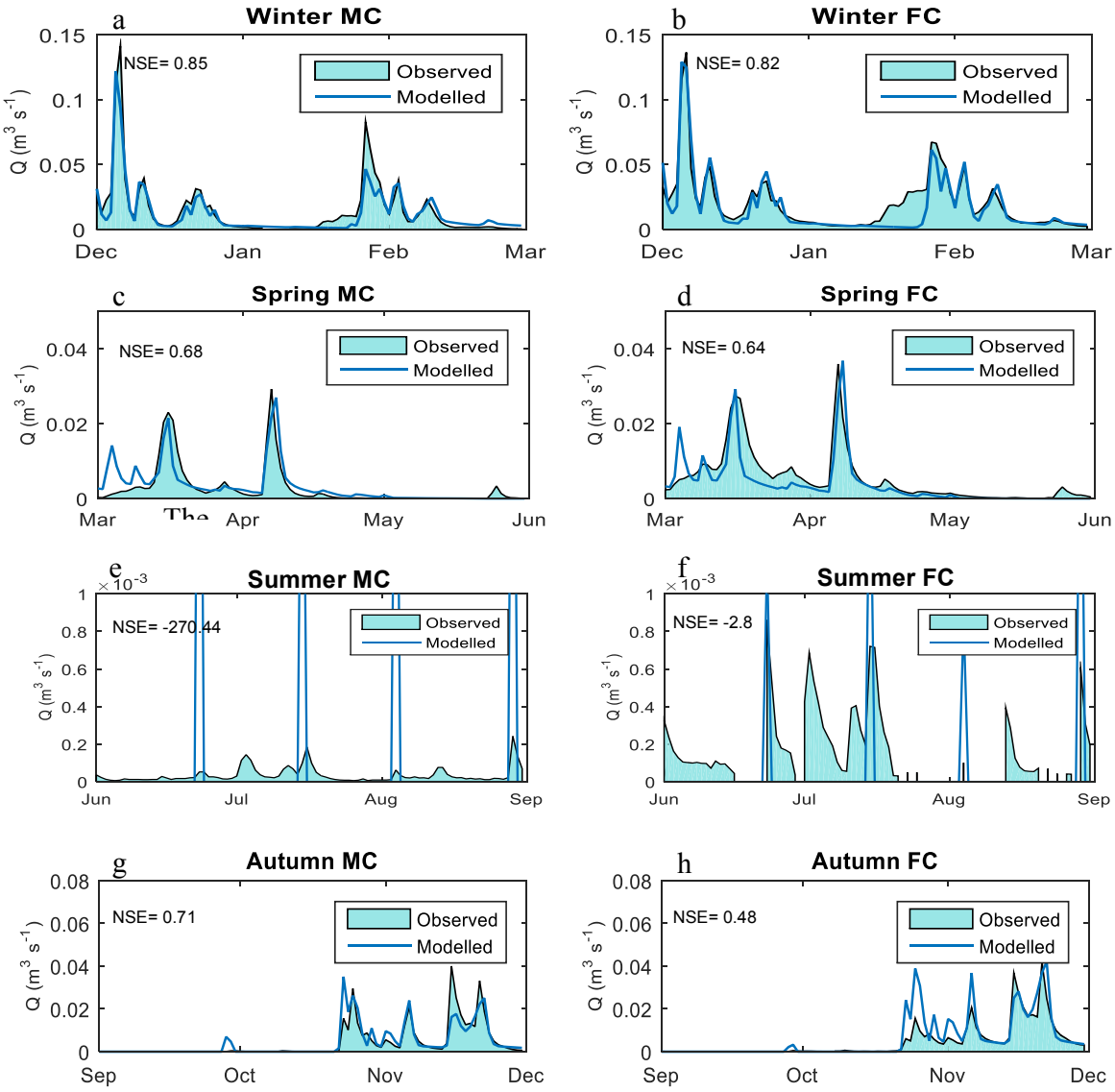

Figure 11. Seasonal variations in HYPE performance for the mire catchment (MC) and the forest catchment (FC) for the period 01-12-2015 to 30-11-2016, compared with observations. a-b) Winter (Dec, Jan, Feb), c-d) Spring (Mar, Apr, May), e-f) Summer (Jun, Jul, Aug), and g-h) Autumn (Sep, Oct, Nov) are presented for both catchments. Note that the y-axis ranges differ between sub-figures due to large seasonal fluctuations in discharge.

The model proved to be most sensitive to the parameter *srrate* (surface runoff rate) (Appendix II), especially for peat and coarse soils. The model was also sensitive to *cevp* (rate for basic PET). The other parameter ranges did not influence model parameter NSE. Rather, another set of parameters could result in the same NSE, which can be concluded by the range of NSE for the same parameter value in (Figure A2 in Appendix II). This means that several combinations of parameters could result in the same calibration NSE.

4.2 Hydrological regime and water balance

4.2.1 Inter- and intra-annual discharge

Average yearly specific discharge decreased with 17% for RCP2.6, RCP4.5 and RCP8.5 relative to MC period 1 (Table 5). Similarly, q (mm d^{-1}) decreased with 12%, 12% and 11%, respectively, for the FC. Average yearly specific discharge was hence very similar for all scenarios (Table 5). Modelled discharge between the two streams for the same climate scenario also showed a large conformity (Wilcoxon's test, $p \leq 0.05$).

The FC had 1.5 times higher yearly specific discharge (mm y^{-1}) than the MC (Table 5) and a larger range and intra-annual fluctuation in q. The ratio between specific discharge of FC and that of MC was hardly affected by the climate change scenarios, it increased from 1.5 to 1.6. Median q was 40% higher for the FC compared to the MC.

Table 5. Average yearly (M) modelled specific discharge**,** range of q and median ($\widetilde{X}$), including standard deviation (σ) for both streams for Period 1 (P1) and period 2 (P2) following RCP2.6, RCP4.5 and RCP8.5, respectively.

		M (mm y^{-1}) (σ)	Range (mm d^{-1}) (σ)	$\widetilde{X}$ (mm d^{-1})
MC	**P1**	242 (61)	0.00 - 17.04 (1.47)	1.65
	RCP2.6	202 (50)	0.00 - 11.90 (0.91)	0.25
	RCP4.5	202 (57)	0.00 - 14.32 (0.91)	0.22
	RCP8.5	202 (48)	0.00 - 12.30 (0.95)	0.17
FC	**P1**	355 (88)	0 - 20.28 (2.13)	2.77
	RCP2.6	311 (70)	0 - 15.61 (1.37)	0.40
	RCP4.5	311 (87)	0 - 18.29 (1.40)	0.35
	RCP8.5	317 (72)	0 - 16.38 (1.49)	0.25

Maximum q, σ and median q was higher for P1 than any scenario in P2 for both catchments, which means that q showed a larger variance in magnitude and frequency in P1. RCP8.5 resulted in a lower median q than RCP2.6 and RCP4.5 compared to similar discharge ranges and σ, suggesting more extreme discharge following RCP8.5. The standard deviation was also higher for RCP8.5. RCP4.5 resulted in the largest range in modelled q and the largest variation in average yearly specific discharge for the 30y period (Figure 12). RCP4.5 had the highest maximum q for both catchments and had a standard deviation for yearly specific discharge more like P1 than the other scenarios.

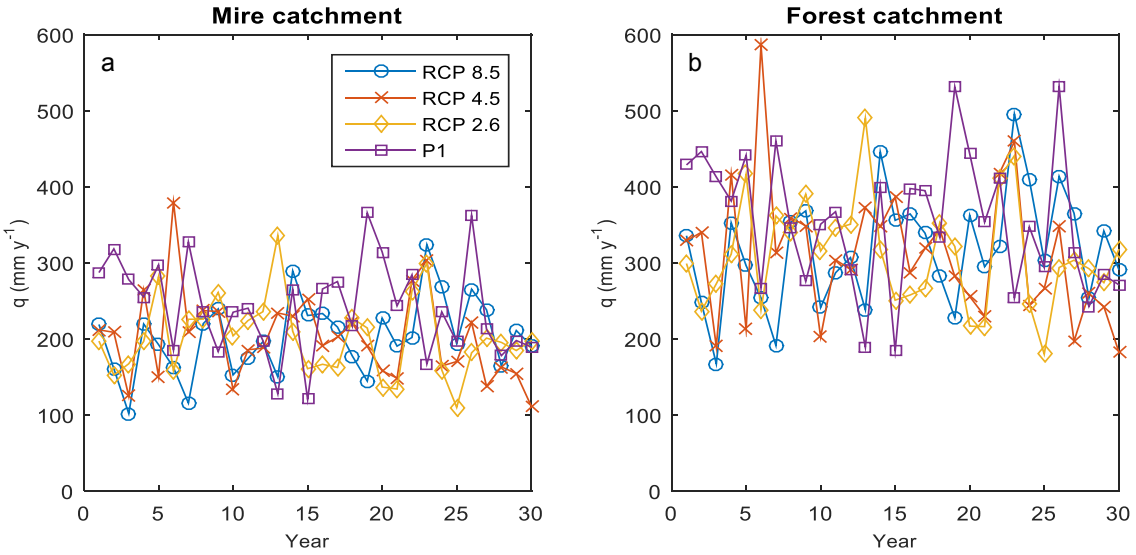

Figure 12. Modelled average yearly specific discharge (mm y^{-1}) including period P1 and P2 for a) mire catchment, and b) forest catchment. MC average *q* was 242 (σ 61) and was 202 (σ 50), 202 (σ 57) and 202 (σ 48) mm y^{-1} following RCP2.6, RCP4.5 and RCP8.5, respectively. FC average *q* was 355 (σ 88) and 311 (σ 70), 311(σ 87) and 317 (σ 72) mm y^{-1} for RCP2.6, RCP4.5 and RCP8.5, respectively.

The spring flood disappeared in the future following all RCP scenarios, shifting the occurrence of peak flow to late autumn and winter (Wilcoxon's test, $p \leq 0.05$) (Figure 13). Summer discharge did not decrease compared to P1 for neither climate scenario (Wilcoxon's test, $p \leq 0.05$). Future intra-annual discharge pattern was consistent following all RCP scenarios, but the FC had a higher intra-annual fluctuation than the MC (Wilcoxon's test, $p \leq 0.05$) (Figure 13).

The intra-annual discharge range for the 30y period narrowed for P2, which means there was a smaller span between minimum and maximum *q* (Figure 14). Figure 14 displays the range only for P1 and RCP8.5 in P2, as all future scenarios produced very similar patterns. However, the pattern differed between the two catchments. The MC had a smaller range of *q*, especially in spring. In P1, the FC showed a large difference in range between June and July, which was not apparent for the MC. Even though average discharge increased in autumn and winter in P2 (all RCP scenarios) (Figure 14), P1 still had a higher maximum *q* for all months expect September for the MC, and August and September for the FC. P1 had a larger discharge variation (1 σ) for both catchments for most months, except for August until November. Comparing σ for RCP8.5, the difference between MC and FC was largest during the non-growing season and decreased in the summer months.

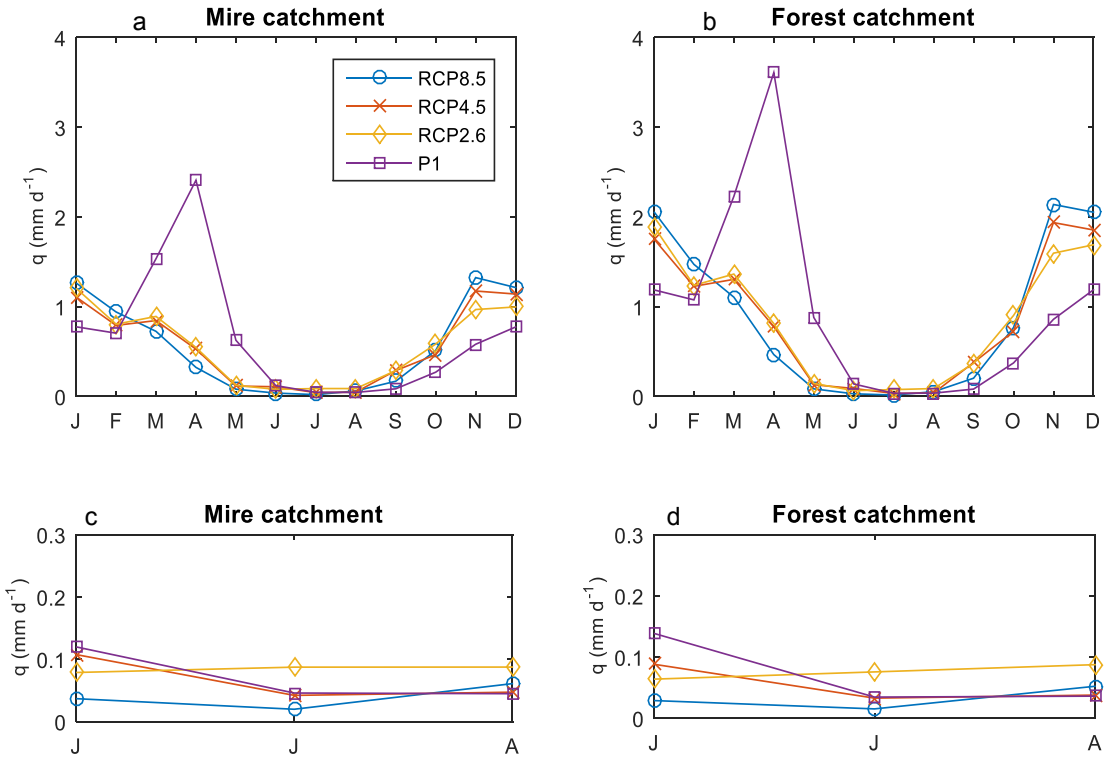

Figure 13. Modelled monthly average specific discharge (q) (mm d^{-1}) for the a) mire, and b) forest catchment, including Period 1 (P1) and Period 2 following RCP2.6, RCP4.5 and RCP8.5, respectively. The lower figures show specific discharge for June, July and August for the c) mire and d) forest catchment.

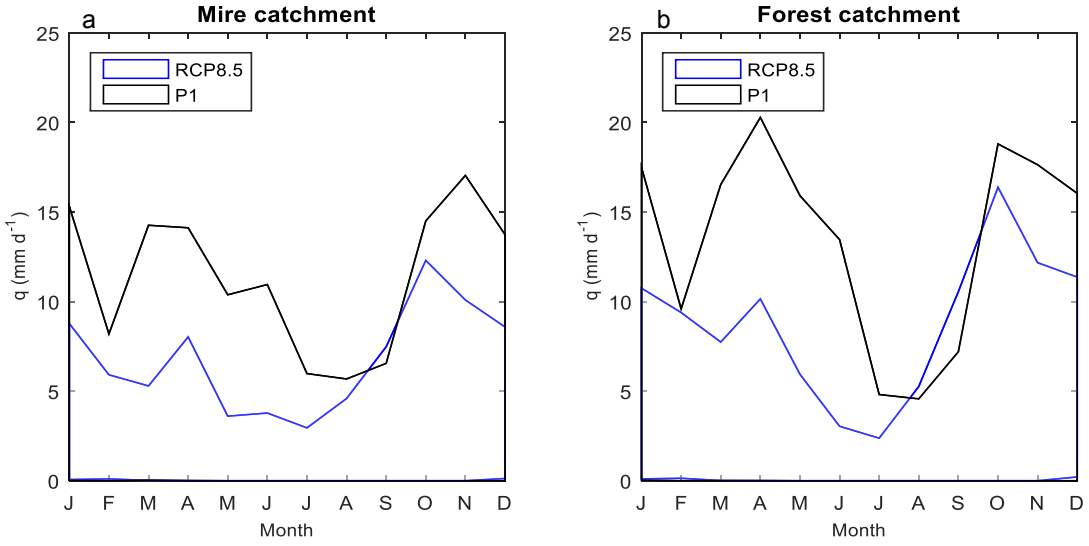

Figure 14. Modelled range in specific discharge (min–max)(mm d^{-1}) for P1 and P2 following RCP8.5 for the a) mire, and b) forest catchment. The maximum q is shown by a black and blue line, respectively. Minimum q is zero or close to zero in all cases.

4.2.2 Water balance

Modelled water balance in P2 was very similar following all climate scenarios. Discharge decreased with ~7% for the MC and ~8% for the FC, following all RCP scenarios (Figure 15). Evapotranspiration increased with ~8% for both catchments following all RCP scenarios. There was also a trend towards reduced water storage for the MC where storage decreased from 340 mm y^{-1} in P1 to 88 mm y^{-1} following RCP8.5. For the FC, water storage could be considered negligible for both periods. There was little or no difference for P2 terms of total storage, discharge or evaporation between climate scenarios.

In the MC, the modeled average yearly soil water storage, i.e. how much water that is held in the soil, decreased with 8%, 8% and 9% compared to P1 following RCP2.6, RCP4.5 and RCP8.5. In the FC, the average yearly water storage decreased with 5%, 5% and 7%, respectively. The summer months had a larger decrease in soil water relative to P1 and the relative decrease for MC was more profound than for the FC, especially in the late autumn and winter (Table 6). RCP8.5 contributed to a larger relative decrease in water storage than did RCP4.5 and RCP2.6.

Table 6. Relative decrease (%) in modelled average water storage for each month relative to P1 in P2 following RCP2.6, RCP4.5 and RCP8.5.

	J	**F**	**M**	**A**	**M**	**J**	**J**	**A**	**S**	**O**	**N**	**D**
RCP8.5												
MC	7%	8%	9%	10%	11%	11%	10%	10%	10%	9%	8%	8%
FC	3%	4%	6%	9%	10%	11%	11%	10%	8%	6%	4%	3%
RCP4.5												
MC	7%	7%	8%	9%	10%	9%	9%	9%	9%	8%	8%	7%
FC	3%	4%	5%	7%	8%	7%	7%	8%	5%	4%	3%	3%
RCP2.6												
MC	6%	7%	7%	9%	9%	9%	9%	8%	8%	7%	7%	7%
FC	3%	3%	5%	7%	7%	7%	6%	6%	4%	2%	2%	2%

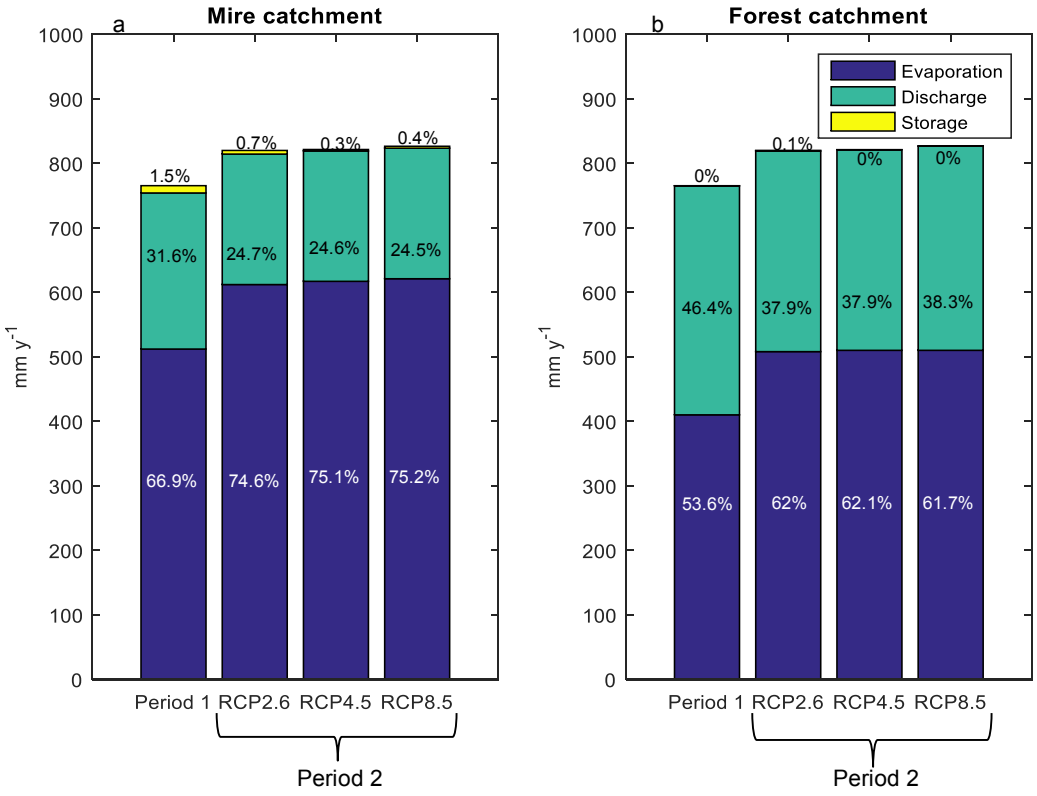

Figure 15. Modelled water mass balance (mm y^{-1}) for P1 and P2 following RCP2.6, RCP4.5 and RCP8.5, respectively, for a) mire catchment, and b) forest catchment. The total height of the bars represents the sum of precipitation. Evaporation, discharge and water storage are presented as a percentage of precipitation.

4.3 DOC concentrations and mass flux

4.3.1 Evaluation of catchment-specific temperature-dependent regression model on DOC concentrations and mass flux

For both sites, T_{avg60} was the most important explaining factor for DOC concentrations, and the only explanatory factor with a significance of ≤ 0.01. T_{avg60} alone could explain 57% for the MC. T, T_{avg60} and T_{avg30} together explained 59% of DOC concentrations from the MC. None of the other variables were significant explanatory factors. For the FC, T_{avg60} alone could explain 65% of DOC concentrations. T, T_{avg60} and T_{avg30} together explained 67% for the FC, whereas for the FC, T_{avg60}, q and q_{-14} together could explain 70% of DOC export. The RMSE was 6.89 mg L^{-1} for the MC and 6.9 mg L^{-1} for the FC (Figure 16). There was a significant correlation between modelled and sampled DOC (mg L^{-1}) for the MC ($\rho = 0.74$, $p \leq 0.01$, $n = 77$, Spearman rho) and the FC ($\rho = 0.67$, $p \leq 0.01$, $n = 63$, Spearman rho).

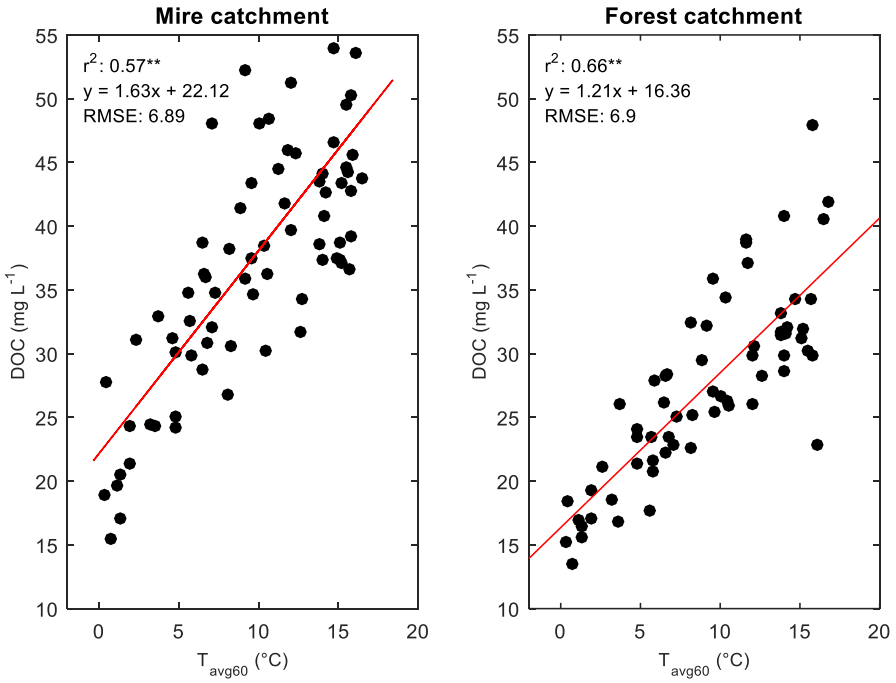

Figure 16. Observed DOC concentration as a function of average air temperature (*T*) 60 days prior to sampling date (denoted T_{avg60}). RMSE is calculated based on [DOC] T_{avg60} for the date of sampling DOC.

Observed DOC concentrations ranged from15.44 to 63.12 mg L^{-1} for the MC and 13.49 to 47.93 mg L^{-1} for the FC. When the model was applied, and compared to monthly concentrations measured at the catchments' outlet, it was clear that measured DOC concentrations showed larger ranges than modelled values for 2012-2016 (Figure 17). Observed winter concentrations were lower than modelled ones, and the model did not fully capture measured peak values during summer and autumn for both catchments. The high DOC concentrations measured in October were sampled during 2013 and 2016, both years recorded warm and dry autumns. These samplings were made after periods of drought, and thus measured concentrations were high as no export had been taken place. This implies that the model did not capture concentrations during flushes succeeding dry periods. This was also evident when DOC for the full period of 2012-2016 was modelled and compared to measured concentrations (Figure A3, Appendix III). However, most measured concentrations were in the range of the modelled ones, except for autumn and winter concentrations for both catchments.

Most modelled concentrations were found in the mid-range of measured concentrations for both catchments (Figure 17). The measured range was larger for the MC and the variation of values measured at the MC was not captured by the model. The FC was overall better captured by the model based on visual inspection. Modelled values were better in line with measured values for the FC during winter, spring and early summer, whereas measured values in late summer and autumn had a larger spread than was captured by the model.

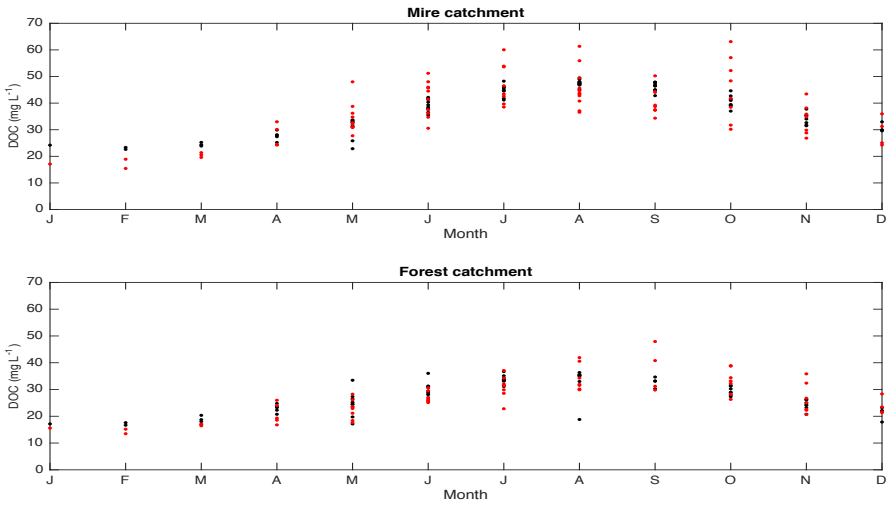

Figure 17. Modelled and measured DOC concentration in 2012-2016. Modelled values are presented as black dots and sampled values as red dots. The modelled values are based on the catchment-specific temperature dependent regression model for each catchment. Modelled values are shown for the same day as the respective corresponding sampling value. In total, there were 77 observations for the mire catchment and 64 observations for the forest catchment.

There was a large variance in measured (2012-2016) DOC mass flux (mg m^{-2} d^{-1}) for all months that had more than a few measured values (Figure 18). Summer and especially October, November and December demonstrated vast variations in export and there was a high average export during these months. The average measured annual export trend was very similar between the catchments, including a peak in April during spring flood.

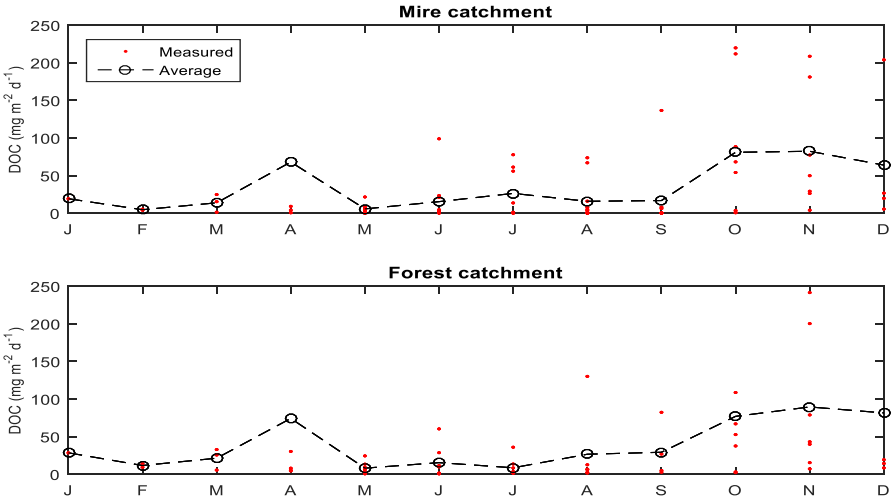

Figure 18. Measured DOC mass flux (mg m^{-2} d^{-1}) as well as the average monthly value based on measurements for each month 2012-2016. The month of April had one measured value of >300 mg m^{-2} d^{-1} (both catchments) not shown in the figure. Also, the month of December had a measured value of 284 mg m^2 d^{-1} (FC) not presented in the figure.

4.3.2 Application of catchment-specific temperature-dependent regression model

Intra-annual export in P1 was similar to the measured average for both catchments (Figure 18, Section 4.3.1). However, the measured export was in October, November and December as large as in April, which was not covered by the model in P1. Modelled export in May was also larger in P1 than measured May export (Figure 19).

The average modelled monthly DOC mass flux demonstrated a changed pattern in P2 following all RCP scenarios relative to P1 (Figure 19). Modelled DOC monthly export was evidently similar to the pattern of average monthly *q* (Figure 14, Section 4.2.1). Hence the modelled DOC export in P2 decreased during spring, but increased during the autumn and winter season compared to P1 (Wilcoxon's test $p \leq 0.05$).

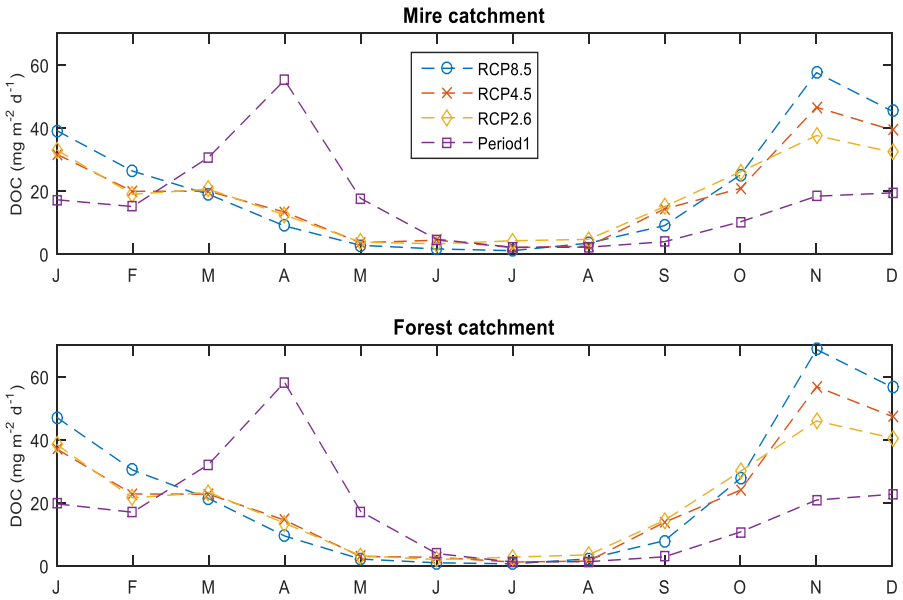

Figure 19. Average modelled monthly export of DOC (mg m^{-2} d^{-1}) following the three different climate scenarios RCP2.6, RCP4.5 and RCP8.5, respectively, for P2 (2071-2100), in addition to P1 (1961-1990).

There was no significant difference in DOC export between P1 and P2 during the summer season (Wilcoxon's test $p \leq 0.05$). Modelled peak DOC export occurred in November or December following all RCP scenarios, which can be compared to current peak concentrations coexisting with the spring flood for P1. RCP8.5 resulted in the highest DOC export rates, occurring in November.

Modelled average yearly export (t C y^{-1}) for the MC increased with 7.7%, 10.9% and 21.3% following RCP2.6, RCP4.5 and RCP8.5, respectively, relative to P1. Average yearly export (t C y^{-1}) for the FC increased with 15%, 19%, 19.5% following RCP2.6, RCP4.5 and RCP8.5, respectively, relative to P1 (Table 7). The FC had a higher modelled specific export than the MC, however differences between catchments were larger during P2 (Figure 20).

Table 7. Modelled DOC export (t C y^{-1}) and (g m^{-2} y^{-1}), including a standard deviation of 12%, from the MC and FC for P1 and P2 following RCP2.6, RCP4.5 and RCP8.5, respectively.

	Period 1		**RCP 2.6**		**RCP 4.5**		**RCP 8.5**	
	MC	FC	MC	FC	MC	FC	MC	FC
t C y^{-1}	3.38	3.05	3.64	3.51	3.75	3.63	4.10	4.04
(± SD)	(0.41)	(0.37)	(0.44)	(0.42)	(0.45)	(0.44)	(0.49)	(0.48)
g C m^{-2} y^{-1}	5.96	6.30	6.43	7.26	6.62	7.50	7.25	8.34
(± SD)	(0.72)	(0.76)	(0.77)	(0.87)	(0.79)	(0.90)	(0.87)	(1.00)

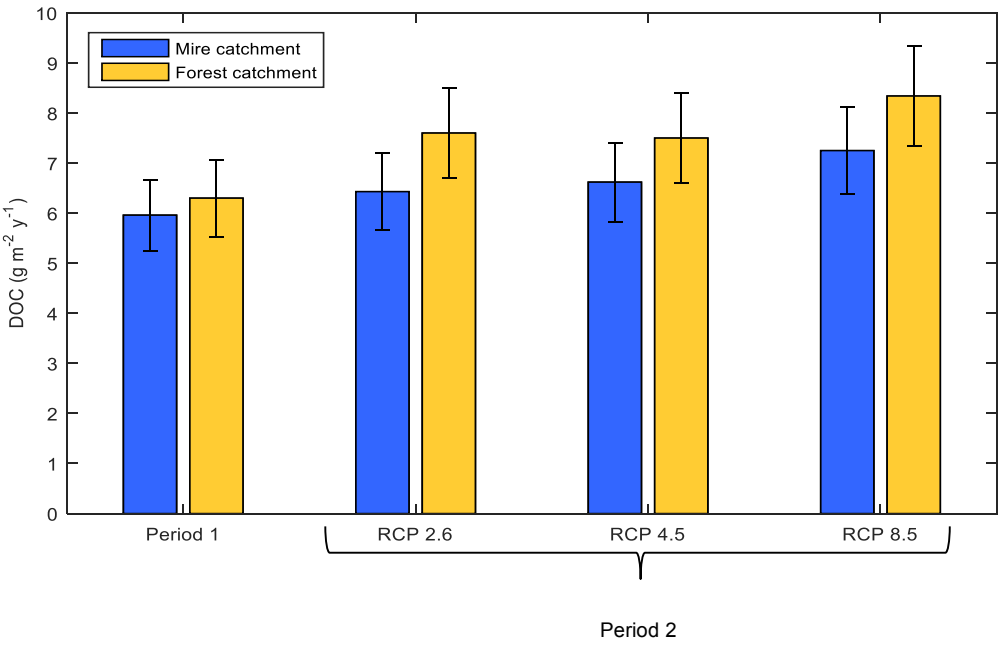

Figure 20. Modelled average annual specific export of DOC (g m^{-2} y^{-1}) from the mire catchment (MC) and the forest catchment (FC). The error bars represent a standard deviation of 12%.

5. DISCUSSION

5.1 HYPE model performance

5.1.1 Model calibration and validation

Hydrological modelling that captures landscape characteristics on a small spatial scale can outline directories for decisions regarding water management and ecological assessments. Small scales facilitate differentiation of model behavior and sources of error. Model calibration and validation is an essential step to understand model processes and areas for improvement.

The model adequately captured discharge dynamics for both catchments. There was in general a large agreement in efficiency and timing between model calibration and validation results for both catchments (NSE and CC), indicating that the model was not over parameterised in the calibration step (Robert et al. 2016).

As the model in general better captured the observed base flow than the observed peak flow, the preferential flow parameters could have been more carefully calibrated in the first step. The very best Monte Carlo simulation after macro-pore calibration (per NSE) was not the one chosen as the final parameter set up, but instead the sixth best simulation, which provided satisfying results on the other model performance criteria as well. This stresses the importance of not optimising just one performance criterion, as all model evaluations are based on an average over the full calibration period, and thus highlights the need of also careful visual inspection of model results, e.g. when evaluating seasonal model performance. Model calibration could have been improved by a proceeding step after the Monte Carlo simulation, using individual parameter model calibration of the most sensitive parameters. However, as the NSE after the final calibration step in this study was high (0.83 for both investigated catchments), this additional procedure was not performed.

Model sensitivity emerges both from forcing input data and model parameter set-up (Arheimer et al. 2012). It was difficult to separate the contribution of errors either to the quality of the input data, missing precipitation and discharge data or the model set-up. Relative bias e.g. decreased substantially for the FC during model validation, from 1.13% to -18.69%, which was likely due to the large gaps in measured precipitation data from April to October in 2015, severely affecting model performance in, inter alia, summer season (Figure 11 and Figure 11f). Precipitation data from nearby whether stations had most likely produced substantial improvement if these had been used as replacement values for missing values.

The MC had considerably lower summer NSE, implying the need of soil layer revision for the peat soil as ET is modelled linearly for the two upper soil layers. The two upper soil layers in the model setup had a total depth of 1.2 m, which means that the model simulates ET down to that level, which is highly unlikely. More detailed soil depth estimations could have been performed during a second visit at the site. The discrepancy in modelled and observed data in early spring (Figure 11c-d) could imply that snowmelt dynamics are not completely captured

by the model and more so for the FC than the MC. Dividing the validation in seasons was a good way to evaluate model processes on a small temporal scale.

Daily resolution data was used in the model set-up. Measured discharge in Skogaryd 2012-2016 had a higher correlation to P_{-1} than P for both catchments, indicating that a daily time step maybe did not capture the temporal response of the relatively small investigated sub-catchments (Ficchì et al. 2016). A sub-daily model resolution would better capture the magnitudes of peaks and would also result in a less tendency of over-parameterisation during model calibration (Ficchì et al. 2016). A sub-daily model resolution could potentially have improved the model outcome, but this would also require a higher temporal resolution of the driving data.

5.1.2 Parameter set-up and model structure

Despite the limitations in measured discharge and precipitation data, the hydrological regime was very well captured by the model for both catchments (Moriasi et al. 2007), meaning that most model parameters were likely well assessed. The model was most sensitive to the parameter *srrate* (surface runoff rate), especially for the thin soil covering the open crop bedrock and the coarse soil (Appendix II). The parameter *srrate* affects the fraction of water that goes into surface runoff and is therefore highly depending on the season. A possible model improvement could involve seasonal values of *srrate*. Also, threshold parameter for snowmelt could be revised as discussed in Section 5.1.1.

Both PET and ET are subjects to uncertainty in water budget calculations in hydrological models (Haddeland et al. 2011). Evaporation is affected by soil layer depths set by the user and was here modelled by the basic ET model (Lindström et al. 2010). Evapotranspiration is based on the land use parameter for basic rate for PET (*cevp*), which was also one of the largest sources to model sensitivity in this study. Parameters involved in PET/ET should ultimately have been revised and/or preferably, another PET/ET model could have been used.

HYPE uses a steady state vegetation cover, and thus does not contain dynamic vegetation. Neither interception, nor leaf area index nor forest stand age were included in the model set-up (Haddeland et al. 2011). Interception, rate for basic PET and snowmelt e.g. are hence assumed to stay consistent also in the late 21st century. In reality, possible clear-cuts and change of vegetation dynamics such as cover, production, bud burst and growing season will all alter with climate change (Valentini et al. 2014), e.g. start of growing season will shift with about -50 days and last for about 3 months longer following RCP8.5 by the end of this century (SMHI 2017c), which severely would affect PET and ET estimations in P2. Including dynamic vegetation could significantly reduce hydrological variability and model uncertainty response to land management and land use change, including climate change induced vegetation changes (Thompson et al. 2014; Xuan et al. 2016).

5.1.3 Climate data and data quality in model application

The more complex the model is, the more it relies on input data quality (Janssen and Heuberger 1995). Each step used in this study; emission scenarios → global circulation model

(GCM) → downscaling approach → bias correction → hydrological modelling, is subject to uncertainty. The here-applied bias correction was an attempt to normalise the downscaled GCM model data to fit observed temperature and precipitation monthly means of Skogaryd. The climate data used was part of a first attempt to regionalise GCM data using statistical methods and the methodology is yet to be refined (Pers. communication, Tinghai Ou, 07-05-2017). Downscaling techniques are identified as central contributors to uncertainties linked to the future hydrological cycle, which is due to the large discrepancy in temporal and spatial resolution to the hydrological model (Xu et al. 2005). Also, the distinctive differences in simulation results between current GCM models provide a great deal of uncertainty (Jiang et al. 2007; Baumberger et al. 2017). The larger discrepancy between current and future climate, the larger the magnitude of parameter bias in the model (Remesan and Holman 2015). The downscaling technique likely caused an attenuation of trends and differences between different scenarios.

5.2 Climate change impact on discharge and water balance

Depending on current and future emission policies, climate change will most likely lead to an intensification of the hydrological cycle including higher amounts and more intense precipitation and increased evaporation (Kjellstrom and Lind 2009). Modelling the hydrological response to climate change on a small-scale favour in depth research about empirical process vital for our understanding of future possible outcomes, and thus provides a foundation for many other science fields involving hydrology.

This study modelled water balance and discharge of a forest and a mire dominated sub-catchment. Climate change will by the end of this century result in to higher winter discharge and detriment of spring flood in the catchments. Specific discharge variation will decrease in magnitude and frequency in the long-term future, per this study. This is in line with findings from similar studies and model approaches for Sweden (Xu 2000; SMHI 2017f). The large difference in modelled median q (mm d^{-1}) between P1 and P2 was most probably due to the changes in future snow melt dynamics. Due to a significant decrease in snow accumulation and warmer temperature, precipitation driven discharge rather than snowmelt driven discharge will increase in the future and peaks in the order of magnitude of the current spring flood will likely disappear (Xu 2000; Vormoor et al. 2016). Instead, there will be more pronounced autumn and winter discharge, as seen from Figure 13.

Average yearly specific discharge decreased with 17% and 11% following all RCP scenarios for the MC and the FC, respectively. However, the precipitation increase here applied for the three RCP scenarios was smaller than the projected precipitation increase in P2 in the Nordic region, which is 5-20% depending on season and scenario (Collins et al. 2013). Estimated precipitation increase in Sweden in P2 is on average 20% for RCP 8.5 (relative to 1971-2000), with a difference of +25% in winter and +10% in the summer (SMHI 2017e), which is to be compared to the driving data of +8%. Precipitation is, due to large spatial and temporal variability, hard to discern (Stocker et al 2013). The climate driving data methodology most likely caused a removal of peak values. As the regional bias correction, somewhat auto-correlated the driving data to fit Skogaryd, it is safe to say that the GCM and downscaling approach did not manage to capture future regional trends. Results from the Sweden

calibrated HYPE model, S-HYPE, instead suggests an alteration of yearly specific discharge in P2 of -5% to +5% (~0%) following RCP4.5 and RCP8.5 (SMHI 2017f).

Observed discharge was ~440 mm y^{-1} for the MC and ~520 mm y^{-1} for the FC in 2012-2016. Yearly modelled specific discharge in P1 was 50-60% and 70-90% of the observed average for the area (400-500 mm y^{-1}) for the MC and FC, respectively (SMHI 2009). Model input *T* and *P* data were measured values for P1 (1961-1990), indicating that the model was somewhat underestimating discharge. The model calibration and validation were based on an observational time series of four years (2013-2016), where 2013 and 2016 were two dry years, likely affecting the model parameter set up. Longer observation time series would have included more representative discharge dynamics for the two catchments and probably produced better estimates of the included parameter values. Also, the "current state" was the reference period 1961-1990. However, observed MAT and MAP has already increased with 1.4 °C and 40% (2012-2016), respectively, relative to P1– which makes P1 a good reference to presumably past conditions but not to the current climate.

A comparison between modelled discharge for P1 and observed discharge (2012-2016) gives that the observed discharge had more and higher peaks due to lower median discharge and larger range, which is a further indication that the MC had a lower observed median than the FC. This suggests that during winter and snowmelt, infiltration is inhibited and surface runoff thus contributes to higher flushes. It is hard to say whether this relationship was captured by the model as this model set up did not include the formation of ice lenses. It is however important to point out that the mire only constituted 40% of the MC.

The FC had a larger average inter-annual and intra-annual modelled discharge range than the MC in P1 (Figure 12 and Figure 13). This could be since the MC is ~17% larger in area than the FC, making the response time to precipitation smaller for the FC, as seen in Table 4 (Grip and Rodhe 1994; Temnerud et al. 2007; Hrachowitz et al. 2010; Lyon et al. 2012). Both the recession coefficient for saturated surface runoff and the fraction for surface runoff was put higher for the FC (Appendix I), which means that a larger portion of the water will go to surface runoff in the FC, thus producing higher average values during the 30y period. Rate for basic PET (*cevp*) was also significantly higher for the mire than the forest (Appendix I). This contributed to the large difference in modelled ET seen in Figure 15 and the relationship between the relative decrease in soil water storage between P1 and P2 for the MC and FC seen in Table 6. If model estimations were correct, average yearly water table could decrease with 25 cm in the MC. Increasing temperatures in the FC during the summer will lead to higher PET, whereas for the MC, it will only to a certain extent affect PET, as the mire is host to plants with shallower root systems (Gong et al. 2012; Mezbahuddin et al. 2016). This further highlights the need of a recalibration of the model, and possible additional adjustments of ET calculations.

Most of the limitations regarding model set up and input data was discussed in Section 5.1. In general, the differences between the two catchments regard the model set up and parameter values, which could have been more carefully studies and evaluated. Model parameters related to macro-pore flow were similar for all soil types, whereas mires during dry periods form macro-pores, which decreases the lag time. The model did also not simulate the

formation of ice-lenses which is an important part of mire runoff. In a more in-depth study, this could have been included. However, this study outlined some difficulties with hydrological modelling as a response to climate change given that the magnitudes of peak discharge and yearly discharge will probably stay consistent. The difficulties involve model-set up, data quality and the interference of the model user. However, it did provide necessary information about how discharge dynamics might alter in a future climate, and strengthens the fact that small-scale modelling needs further scientific notion.

5.3 DOC concentrations and mass flux

Export of DOC is governed by hydrology and the aquatic-terrestrial connectivity of DOC from foremost mires but also forests is a significant factor when estimating the response of aquatic ecosystems to climate change (Pastor et al. 2003). As the intra-annual variability of DOC export was large, research on small scale is needed to provide a better understanding of controlling factors.

The model could explain 57% of DOC concentration for the MC and 65% for the FC, which is higher than some other statistical analysis on DOC (Hytteborn et al. 2015). The MC had a faster temperature response (steeper slope in Figure 16), which is in line with a similar study on the catchments (Wallin et al. 2015). Mires usually display a strong temperature control, whereas DOC export from hemi-boreal forests is more governed by the hydrological regime where the organic content usually decreases with depth. In the FC, the sampling point (outlet) is located downstream the former agricultural area consisting of various clay and silt minerals with little vertical heterogeneity. Large parts of the drainage system are also located here, meaning a large stream-riparian zone interface in this area. This could also suggest that this is a wet area. Even if DOC can adsorb to clay particles, the former agricultural land use probably added organic material to the soil. In a podzol, below the O-horizon (the top organic soil layer), water flux have proved to have limited control on DOC export due to sorption-desorption processes and more homogenous carbon concentrations (Fröberg et al. 2006). Hence, for both investigated catchments, the T_{avg60} control on stream DOC was likely a control on the production, and not the mobilisation (Wallin et al. 2015; Porcal et al. 2009). The here observed temperature lag has also previously been found for the O-horizon in forest catchments in Sweden (Fröberg et al. 2006).

The linear regression-model approach was an attempt to model inter-annual variations of DOC using correlations to available observational data of temperature, discharge and precipitation. Both catchments proved to have strong correlation with T_{avg60}, which can be the interpreted as the soil temperature (Ågren et al. 2008; Winterdahl et al. 2016). Soil temperature has been identified as an important control in modelling DOC concentration seasonality (Hytteborn et al. 2015). Temperature directly affects DOC production as decomposition and mineralisation rates are governed by temperature (Hope et al. 1994). Indirectly, temperature affects DOC production by affecting net primary production and growing season. Increasing temperatures also affects season length and evapotranspiration which in turn governs soil moisture. The study modelled increasing DOC concentrations and export in P2 following all climate scenarios due to increasing MAT. A recent study found that temperature had a strong control over DOC concentrations, however they found an optimum

of DOC concentrations at MAT 0-3 °C in boreal and hemi-boreal streams – temperatures above this threshold result in increased mineralisation (Laudon et al. 2012). However, in a mire where the conditions are mostly anaerobic the mineralisation process is slowed down, the temperature optimum range could possibly expand. The model was due to above mentioned reasons not considered suitable to model future DOC concentration and export. Even though the measured values were few, there was a larger intra-annual than inter-annual trend. Modelled concentrations were lower than observed during the growing season, which is a clear indication that the model did not capture the catchments' complexity and sensitivity to DOC production and mobilisation, especially for the MC.

The model was based on DOC seasonal dynamics. However, over the seasons, environmental factors like soil moisture, precipitation and water fluxes, freezing/thawing, nutrient availability and land-use management along with chemical properties of the soil affect DOC production and mobilisation (Pind et al. 1994; Kalbitz et al. 2000; Pagano et al. 2014). These factors were not included in the study but some of them are related to soil temperature. Likely, the high temperature correlation was likely a correlation to DOC production factors related to temperature.

Increasing MAT and decreasing WT for the MC as modelled in this study, could lead to lower stream DOC concentration as this allow full decomposition of organic matter. Given the modelled water balance, that did not decrease for the FC in this study, and steady state vegetation, DOC concentrations would not necessarily decrease for the FC (Lyon et al. 2011).

Given the identified future trend towards a diminishing spring flood as well as higher autumn and winter discharge, intra-annual DOC export dynamics in P2 could be like the modelled trend in the non-growing season. As seasonal trends in DOC export coincide with hydrological flows, and especially extreme events future peak export will likely occur in autumn/winter after the growing season where DOC production is amplified (Wilson et al. 2013). However, due to the large uncertainties regarding peat soil response to climatic drivers and subsequently the soils' hydraulic properties, export patters from MC cannot be delineated.

The main limitation of this study includes the fact that measured values were very few and not evenly spread throughout the year. Using a linear regression approach based on one explanatory variably constitutes inherent inadequacy but provided useful insights on DOC production and mobilisation in both the forest and the mire catchment as a high explanatory factor for DOC concentration was found. Including more explanatory factors could further increase the scientific understanding of the catchments. However, the coupled variation of the hydrologic and biogeochemical systems implies that simple approaches cannot predict DOC concentrations and export in a changing climate (Davidson and Janssens 2006; Lyon et al. 2011).

The results from this study reinforces general findings that no long-term future trends of DOC concentration and export can be defined (Winterdahl et al. 2014a; Winterdahl et al. 2014b). Most likely, a combination of temperature, precipitation and notably environmental drivers that affect net primary productivity will govern DOC production and mobility in the long-term future (Freeman et al. 2004). Further studies are needed on how substrate availability for podzol and peat soil is related to these drivers, coupled with decomposition controls.

6. CONCLUSIONS

The aims of this thesis were to model discharge dynamics and water balance in two characteristically different sub-catchments and the impact of climate change by applying the hydrological model HYPE 4.13.2. Further, the study aimed at linking measured regulating factors on the DOC aquatic-terrestrial connectivity to the modelled hydrological regime to outline a trend for long-term trajectory on future DOC export. Based on the research questions, the study came up with the following conclusions:

1. *Is HYPE applicable for modelling the hydrological regime from both sub-catchments in terms of quantity and dynamics?*

Yes. Both base flow and peak flow was well captured by the model for both the mire catchment and the forest catchment. The model performed well during winter, spring and autumn but did not capture summer dynamics. In conclusion, small temporal and spatial scales facilitate differentiation of model behavior and sources of error.

2. *How will climate change affect future water balance, and what is the difference between climate scenarios?*

Yearly average specific discharge in the long-term future will likely not alter considerably compared to today. No differentiation in response between different climate scenarios could be outlined in the study apart from that extreme events will increase following RCP 8.5. Intra-annual discharge will alter in the long-term future. Spring discharge will attenuate and autumn and winter discharge will increase for both catchments, with a larger intra-annual variation in discharge magnitude for the forest catchment. Water storage for the mire might decrease, affecting the hydrology in the mire catchment.

3. *What is the controlling factor for DOC concentrations for both sub-catchments, and would it be possible to quantify long-term concentrations and mass flux?*

DOC concentrations for the forest catchment were better captured than for the mire catchment. Both catchments proved a very strong temperature control to DOC concentration. The strong temperature control is linked to other abiotic and biotic factors controlling DOC production. The model therefore captured DOC production rather than mobilisation. It was not possible to quantify long-term concentrations and mass flux of DOC; however, export will likely follow that of specific discharge. A simple linear regression model cannot be used for prediction of concentrations and export. The dynamics and interactions governing the DOC production and the aquatic-terrestrial connectivity must be further mapped and linked to soil matrix characteristics and hydrological response to climate change before potential impact of changes in climatic drivers can be outlined.

REFERENCES

Ågren, A., I. Buffam, M. Berggren, K. Bishop, M. Jansson, and H. Laudon. 2008. Dissolved organic carbon characteristics in boreal streams in a forest-wetland gradient during the transition between winter and summer. *Journal of Geophysical Research. Biogeosciences,* 113**:** n/a.

Ågren, A., I. Buffam, M. Jansson, and H. Laudon. 2007. Importance of seasonality and small streams for the landscape regulation of dissolved organic carbon export. *Journal of Geophysical Research. Biogeosciences,* 112**:** n/a.

Amatya, D., T. M. Williams, L. Bren, and C. d. Jong. 2016. *Forest hydrology : processes, management and assessment*. Wallingford : CABI, 2016.

Ashman, M. R., and G. Puri. 2002. *Essential Soil Science - A clear and concise introduction to soil science* Oxford: Blackwell Science Ltd.

Baumberger, C., R. Knutti, and G. Hirsch Hadorn. 2017. Building confidence in climate model projections: an analysis of inferences from fit. *WIREs: Climate Change,* 8**:** n/a.

Chen, D., C. Achberger, T. Ou, U. Postgård, A. Walther, and Y. Liao. 2015. Projecting Future Local Precipitation and Its Extremes for Sweden. *Geografiska Annaler Series A: Physical Geography,* 97**:** 25.

Clark, M. P., D. Kavetski, and F. Fenicia. 2011. Pursuing the method of multiple working hypotheses for hydrological modeling. *Water Resources Research,* 47**:** 16.

Collier, M. A., S. J. Jeffrey, L. D. Rotstayn, K. K.-H. Wong, S. M. Dravitzki, C. Moeseneder, C. Hamalainen, J. I. Syktus, et al. 2011. The CSIRO-Mk3.6.0 Atmosphere-Ocean GCM: participation in CMIP5 and data publication. In *19th International Congress on Modelling and Simulation*. Perth, Australia.

Collins, M., R. Knutti, J. Arblaster, J.-L. Dufresne, T. Fichefet, P. Friedlingstein, X. Gao, W. J. Gutowski, et al. 2013. Long-term Climate Change: Projections, Commitments and Irreversibility. In *Climate Change 2013: The Physical Science Basis. Contribution of Working Group I to the Fifth Assessment Report of the Intergovernmental Panel on Climate Change,* eds. T. F. Stocker, D. Qin, G.-K. Plattner, M. Tignor, S. K. Allen, J. Boschung, A. Nauels, Y. Xia, V. Bex, and P. M. Midgley, 1029–1136. Cambridge, United Kingdom and New York, NY, USA: Cambridge University Press.

Crowther, T. W., K. E. O. Todd-Brown, C. W. Rowe, W. R. Wieder, J. C. Carey, M. B. Machmuller, B. L. Snoek, S. Fang, et al. 2016. Quantifying global soil carbon losses in response to warming. *Nature [London],* 540**:** 104-108. DOI: 10.1038/nature20150

Davidson, E. A., and I. A. Janssens. 2006. Temperature sensitivity of soil carbon decomposition and feedbacks to climate change. *Nature,* 440**:** 165-173.

Dinsmore, K. J., M. F. Billett, and K. E. Dyson. 2013. Temperature and precipitation drive temporal variability in aquatic carbon and GHG concentrations and fluxes in a peatland catchment. *GLOBAL CHANGE BIOLOGY,* 19**:** 2133-2148.

Donnelly, C., W. Yang, and J. Dahné. 2014. River discharge to the Baltic Sea in a future climate. *Climatic Change,* 122**:** 157-170. DOI: 10.1007/s10584-013-0941-y

Efstratiadis, A., I. Nalbantis, and D. Koutsoyiannis. 2015. Hydrological modelling of temporally-varying catchments: facets of change and the value of information. *Hydrological Sciences Journal,* 60**:** 1438-1461. DOI: DOI: 10.1080/02626667.2014.982123.

Freeman, C., N. Fenner, N. J. Ostle, H. Kang, D. J. Dowrick, B. Reynolds, M. A. Lock, D. Sleep, et al. 2004. Export of dissolved organic carbon from peatlands under elevated carbon dioxide levels. *Nature,* 430**:** 195-198.

Freeman, C., N. Fenner, and A. H. Shirsat. 2012. Peatland geoengineering: an alternative approach to terrestrial carbon sequestration. *Philosophical Transactions of the Royal Society A (Mathematical, Physical and Engineering Sciences),* 370**:** 4404-4421. DOI: DOI: 10.1098/rsta.2012.0105.

Gärdenas, A. I., J. Simunek, N. Jarvis, and M. T. van Genuchten. 2006. Two-dimensional modelling of preferential water flow and pesticide transport from a tile-drained field. *Journal of Hydrology* 329**:** 647-660.

Gong, J., K. Wang, S. Kellomäki, C. Zhang, P. J. Martikainen, and N. Shurpali. 2012. Modeling water table changes in boreal peatlands of Finland under changing climate conditions. *Ecological Modelling,* 244**:** 65-78. DOI: 10.1016/j.ecolmodel.2012.06.031

Grip, H., and A. Rodhe. 1994. *Vattnes väg från regn till bäck* Uppsala: Hallgren & Fallgren Studieförlag AB.

Hagemann, S., C. Chen, D. B. Clark, S. Folwell, S. N. Gosling, I. Haddeland, N. Hanasaki, J. Heinke, et al. 2012. Climate change impact on available water resources obtained using multiple global climate and hydrology models. *Earth System Dynamics Discussions, Vol 3, Iss 2, Pp 1321-1345 (2012)***:** 1321. DOI: 10.5194/esdd-3-1321-2012

Hankin, B., S. Bielby, L. Pope, and J. Douglass. 2016. Catchment-scale sensitivity and uncertainty in water quality modelling. *Hydrological Processes,* 30**:** 4004-4018.

Hartge, K.-H., and R. Horn. 2016. *Essential Soil Phydiscs - An introduction to soil processes, functions, strucutre and mechanics*. Stuttgart: Schweizerbart'sche Verlagsbuchhandlung.

Hartmann, D. L., A. M. G. Klein Tank, M. Rusticucci, L. V. Alexander, S. Brönnimann, Y. Charabi, F. J. Dentener, E. J. Dlugokencky, et al. 2013. Observations: Atmosphere and Surface. In *Climate Change 2013: The Physical Science Basis. Contribution of Working Group I to the Fifth Assessment Report of the Intergovernmental Panel on Climate Change,* eds. T. F. Stocker, D. Qin, G.-K. Plattner, M. Tignor, S. K. Allen, J. Boschung, A. Nauels, Y. Xia, V. Bex, and P. M. Midgley, 159–254. Cambridge, United Kingdom and New York, NY, USA: Cambridge University Press.

Holden, J. 2005. Peatland hydrology and carbon release; why small-scale process matters. *Philosophical Transactions - Royal Society. Mathematical, Physical and Engineering Sciences,* 363**:** 2891-2913. DOI: 10.1098/rsta.2005.1671

Holden, J., and T. P. Burt. 2002. Laboratory experiments on drought and runoff in blanket peat. *European Journal of Soil Science,* 53**:** 675-689.

Hope, D., M. F. Billett, and M. S. Cresser. 1994. A review of the export of carbon in river water; fluxes and processes. *Environmental Pollution [1987],* 84**:** 301-324.

Hrachowitz, M., C. Soulsby, D. Tetzlaff, and M. Speed. 2010. Catchment transit times and landscape controls-does scale matter? *Hydrological Processes,* 24**:** 117-125. DOI: DOI: 10.1002/hyp.7510.

Hruska, J., P. Kram, W. H. McDowell, and F. Oulehle. 2009. Increased Dissolved Organic Carbon (DOC) in Central European Streams is Driven by Reductions in Ionic Strength Rather than Climate Change or Decreasing Acidity. *ENVIRONMENTAL SCIENCE & TECHNOLOGY,* 43**:** 4320-4326.

Hundecha, Y., B. Arheimer, C. Donnelly, and I. Pechlivanidis. 2016. A regional parameter estimation scheme for a pan-European multi-basin model. *Journal of Hydrology: Regional Studies,* 6**:** 90-111. DOI: 10.1016/j.ejrh.2016.04.002

Hwang, S., and W. D. Graham. 2014. Assessment of Alternative Methods for Statistically Downscaling Daily GCM Precipitation Outputs to Simulate Regional Streamflow. *Journal of the American Water Resources Association,* 50**:** 1010-1032. DOI: 10.1111/jawr.12154

IPCC. 2013. *Climate Change 2013: The Physical Science Basis. Contribution of Working Group I to the Fifth Assessment Report of the Intergovernmental Panel on Climate Change*. Cambridge, United Kingdom and New York, NY, USA: Cambridge University Press.

Janssen, P. H. M., and P. S. C. Heuberger. 1995. Calibration of process-oriented models. *Ecological Modelling,* 83**:** 55-66. DOI: 10.1016/0304-3800(95)00084-9

Jiang, T., Y. D. Chen, C.-y. Xu, X. Chen, X. Chen, and V. P. Singh. 2007. Comparison of hydrological impacts of climate change simulated by six hydrological models in the

Dongjiang Basin, south China. *Journal of Hydrology,* 336**:** 316-333. DOI: 10.1016/j.jhydrol.2007.01.010

Kalbitz, K., S. Solinger., J. H, Park., B. Michalzik., E. Matzner. 2000. Controls on the dynamics of dissolved organic matter in soils: A review. *Soil Science.* 165: 277-231.

Kane, E. S., L. R. Mazzoleni., C. J. Kratz., J. A Hribljan., C. P, Johnson., T. G. Pypker., R. Chimner. 2014. Peat pore water dissolved organic carbon concentration and lability increase with warming; a field temperature manipulation experiment in a poor-fen. *Biogeochemistry*. 119(1-3): 161-178.

Kasurinen, V., K. Alfredsen, A. Ojala, J. Pumpanen, G. A. Weyhenmeyer, M. N. Futter, H. Laudon, and F. Berninger. 2016. Modeling nonlinear responses of DOC transport in boreal catchments in Sweden. *Water Resources Research,* 52**:** 4970-4989. DOI: 10.1002/2015WR018343

Koch, J., S. Stisen, T. Cornelissen, B. Diekkrüger, Z. Fang, H. Bogena, and S. Kollet. 2016. Inter-comparison of three distributed hydrological models with respect to seasonal variability of soil moisture patterns at a small forested catchment. *Journal of Hydrology,* 533**:** 234-249. DOI: 10.1016/j.jhydrol.2015.12.002

Kokorite, I., M. Klavins, and V. Rodinov. 2010. Impact of catchment properties on aquatic chemistry in the rivers of Latvia. *Hydrology Research,* 41**:** 320-329.

Laudon, H., M. Berggren, A. Ågren, I. Buffam, K. Bishop, T. Grabs, M. Jansson, and S. Köhler. 2011. Patterns and Dynamics of Dissolved Organic Carbon (DOC) in Boreal Streams: The Role of Processes, Connectivity, and Scaling. In *Ecossytems*, 880-893. Springer Science+Business Media.

Laudon, H., and I. Buffam. 2008. Impact of changing DOC concentrations on the potential distribution of acid sensitive biota in a boreal stream network. *Hydrology and Earth System Sciences, Vol 12, Iss 2, Pp 425-435 (2008)***:** 425.

Laudon, H., J. Buttle, S. K. Carey, J. McDonnell, K. McGuire, J. Seibert, J. Shanley, C. Soulsby, et al. 2012. Cross-regional prediction of long-term trajectory of stream water DOC response to climate change. *Geophysical Research Letters,* 39.

Laudon, H., V. Sjoblom, I. Buffam, J. Seibert, and M. Morth. 2007. The role of catchment scale and landscape characteristics for runoff generation of boreal streams. *Journal of Hydrology,* 344**:** 198-209. DOI: 10.1016/j.jhydrol.2007.07.010

Lindström, G., C. Pers, J. Rosberg, J. Stromqvist, and B. Arheimer. 2010. Development and testing of the HYPE (Hydrological Predictions for the Environment) water quality model for different spatial scales. *Hydrology Research,* 41**:** 295-319.

Lyon, S. W., T. Grabs, H. Laudon, K. H. Bishop, and J. Seibert. 2011. Variability of groundwater levels and total organic carbon in the riparian zone of a boreal catchment. *Journal of Geophysical Research,* 116**:** @CitationG01020-@CitationG01020. DOI: 10.1029/2010JG001452

Lyon, S. W., M. Nathanson, A. Spans, T. Grabs, H. Laudon, J. Temnerud, K. H. Bishop, and J. Seibert. 2012. Specific discharge variability in a boreal landscape. *Water Resources Research,* 48**:** n/a-n/a. DOI: 10.1029/2011WR011073

Maurer, EP. 2007. Uncertainty in hydrologic impacts of climate change in the Sierra Nevada, California, under two emissions scenarios. *Climatic Change*, 82: 309-325.

McGlynn, B., J. McDonnell., M. Stewart., J. Seibert. 2003. On the relationships between catchment scale and streamwater mean residence time. *Hydrological Processes*, 17: 175-181.

Meyer, A., L. Tarvainen, A. Nousratpour, R. G. Björk, M. Ernfors, K. Kasimir, Å, A. Lindroth, M. Räntfors, et al. 2013. A fertile peatland forest does not constitute a major greenhouse gas sink. *Biogeosciences Discussions, Vol 10, Iss 3, Pp 5107-5148 (2013)***:** 5107. DOI: 10.5194/bgd-10-5107-2013

Mezbahuddin, M., R. F. Grant, and L. B. Flanagan. 2016. Modeling hydrological controls on variations in peat water content, water table depth, and surface energy exchange of a boreal western Canadian fen peatland. *Journal of Geophysical Research: Biogeosciences,* 121**:** 2216-2242. DOI: 10.1002/2016JG003501

Milly, P. C. D., and P. S. Eagleson. 1988. Effect of storm scale on surface runoff volume. *Water Resources Research,* 24**:** 620-624.

Moriasi, D. N., J. G. Arnold, M. W. Van Liew, R. L. Bingner, R. D. Harmel, and T. L. Veith. 2007. Model Evaluation Guidelines for Systematic Quantification of Accuracy in Watershed Simulations. *American Society of Agricultural and Biological Engineers* 50**:** 885-900.

Munthe et al., J., 2014. Climate change and environmental objectives, Report to Swedish Environmental Agency for 2015 evaluation of environmental objectives. (In Swedish, Klimatförändringar och miljömålen). Especially Gärdenäs A., Rappe George M., Temnerud J., Bishop K., Lindström G., Pers Ch., Strömqvist J., Arheimer B., Moldan F., Juttesträm S., Hytteborn J. Chapter 5.1 and 5.2 Leaching processes at the interface terrestrial and aquatic systems pp 75-81., Naturvårdsverket, Report 6705196 pp. [in Swedish, English summary]

Nash, J. E., and J. V. Sutcliffe. 1970. River flow forecasting through conceptual models; Part I, A discussion of principles. *Journal of Hydrology,* 10**:** 282-290.

Nilsson, M., J. Sagerfors, I. Buffam, H. Laudon, T. Eriksson, A. Grelle, L. Klemedtsson, P. Weslien, et al. 2008. Contemporary carbon accumulation in a boreal oligotrophic minerogenic mire - a significant sink after accounting for all C-fluxes. *Global Change Biology***:** 2317. DOI: 10.1111/j.1365-2486.2008.01654.x

Olefeldt, D., K. J. Devito, and M. R. Turetsky. 2013. Sources and fate of terrestrial dissolved organic carbon in lakes of a Boreal Plains region recently affected by wildfire. *Biogeosciences, Vol 10, Iss 10, Pp 6247-6265 (2013)***:** 6247. DOI: 10.5194/bg-10-6247-2013

Ortiz, C. A., J. Liski, A. I. Gärdenäs, A. Lehtonen, M. Lundblad, J. Stendahl, G. I. Ågren, and E. Karltun. 2013. Soil organic carbon stock changes in Swedish forest soils—A comparison of uncertainties and their sources through a national inventory and two simulation models. *Ecological Modelling***:** 221. DOI: 10.1016/j.ecolmodel.2012.12.017

Pagano, T., B. Morgan., K, E. Jonathan. 2014. Trends in Levels of Allochthonous Dissolved Organic Carbon in Natural Water: A Review of Potential Mechanisms under a Changing Climate. *Water*, 6 (10): 2862-2897.

Parent, L.-E., and P. Illnicki. 2003. *Organic soils and peat materials for sustainable agriculture*. Boca Raton: CRC Press LLC.

Pechlivanidis, I. G., J. Olsson, T. Bosshard, D. Sharma, and K. C. Sharma. 2015. Assessment of the climate change impacts on the water resources of the Luni region, India. *Global Nest Journal,* 17**:** 29-40.

Pers, C., J. Temnerud, and G. Lindström. 2016. Modelling water, nutrients, and organic carbon in forested catchments: A HYPE application. *Hydrological Processes,* 30**:** 3252-3273. DOI: 10.1002/hyp.10830

Pham, H. X., A. Y. Shamseldin, and B. W. Melville. 2015. Assessment of Climate Change Impact on Water Balance of Forested and Farmed Catchments. *Journal of Hydrologic Engineering,* 20**:** 04015009. DOI: DOI: 10.1061/(ASCE)HE.1943-5584.0001169.

Pind, A., C. Freeman., M. A. Lock. 1994. Enzymatic degradation of phenolic materials in peatlands – Measurements of phenol oxidase acitivty. *Plant Soil.* 159: 227-231.

Remesan, R., and I. P. Holman. 2015. Effect of baseline meteorological data selection on hydrological modelling of climate change scenarios. *Journal of Hydrology,* 528**:** 631-642. DOI: 10.1016/j.jhydrol.2015.06.026

Reshmidevi, T. V., D. Nagesh Kumar, R. Mehrotra, and A. Sharma. 2017. Estimation of the climate change impact on a catchment water balance using an ensemble of GCMs. *Journal of Hydrology*. DOI: 10.1016/j.jhydrol.2017.02.016

Porcal, P., J. F. Koprivnjak., L.A. Molot., P.J. Dillon. 2009. Humic substances part 7: The biogeochemistry of dissolved organic carbon and its interactions with climate change. *Envioron. Sci. Pollut. Res.* 16: 714-726.

Shrestha, B., T. A. Cochrane., B. S. Caruso., M. E. Arias., T Piman. 2016. Uncertainty in flow and sediment projections due to future climate scenarios for the 3S Rivers in the Mekong Basin. *Journal of Hydrology*, 540: 1088-1104.

Simunek, J., N. J. Jarvis, M. T. van Genuchten, and A. Gardenas. 2003. Review and comparison of models for describing non-equilibrium and preferential flow and transport in the vadose zone. *Journal of Hydrology,* 272**:** 14-35.

SITES. Swedish Infrastructure for Ecosystem Services. www.fieldsites.se/en-GB

SMHI. 2009. Normal årsavrinning. Retrieved 2 June 2017, fromhttps://www.smhi.se/klimatdata/hydrologi/vattenforing/normal-arsavrinning-1.7967

SMHI. 2017a. Öppna data – Lufttemperatur dygnsvärde. Retrieved 03 March 2017, from https://opendata-download-metobs.smhi.se/explore

SMHI. 2017b. Nederbördsmängd, dygnvärde. Retrieved 03 March 2017, fromhttps://opendata-download-metobs.smhi.se/explore

SMHI. 2017c. Klimatscenarier, vegetationsperiodens längd. Retrieved 10 June 2017, from https://www.smhi.se/klimat/framtidens-klimat/klimatscenarier

SMHI. 2017d. Klimatscenarier, Temperatur. Retrieved 11 June 2017, from https://www.smhi.se/klimat/framtidens-klimat/klimatscenarier

SMHI. 2017e. Klimatscenarier, Nederbörd. Retrieved 11 June 2017, from https://www.smhi.se/klimat/framtidens-klimat/klimatscenarier.

SMHI. 2017f. Klimatscenarier, Länsvisa klimatanalyser, lokal årsmedeltillrinning. Retrieved14 June 2017, from https://www.smhi.se/klimat/framtideklimat/lansanalyser#14_Vastra_Gotaland,HBVS_intrans_MQloc,ANN

Soto-Varela, F., M. L. Rodriguez-Blanco, M. M. Taboada-Castro, and M. T. Taboada-Castro. 2014. Identifying environmental and geochemical variables governing metal concentrations in a stream draining headwaters in NW Spain. *APPLIED GEOCHEMISTRY,* 44**:** 61-68.

Stocker, T. F., D. Qin, G.-K. Plattner, L. V. Alexander, S. K. Allen, N. L. Bindoff, F.-M. Bréon, J. A. Church, et al. 2013. Technical Summary. In *Climate Change 2013: The Physical Science Basis. Contribution of Working Group I to the Fifth Assessment Report of the Intergovernmental Panel on Climate Change,* eds. T. F. Stocker, D. Qin, G.-K. Plattner, M. Tignor, S. K. Allen, J. Boschung, A. Nauels, Y. Xia, V. Bex, and P. M. Midgley, 33–115. Cambridge, United Kingdom and New York, NY, USA: Cambridge University Press.

Strömqvist, J., B. Arheimer, J. Dahnné, C. Donnelly, and G. Lindström. 2012. Water and nutrient predictions in ungauged basins: set-up and evaluation of a model at the national scale. *Hydrological Sciences Journal,* 57**:** 229-247. DOI: DOI: 10.1080/02626667.2011.637497.

Sucker, C., and K. Krause. 2010. Increasing dissolved organic carbon concentrations in freshwaters: what is the actual driver? (Increasing dissolved organic carbon concentrations in freshwaters: what is the actual driver?). *iForest - Biogeosciences and Forestry,* 3**:** 106-108. DOI: 10.3832ifor0546-003

Temnerud, J., J. Seibert, M. Jansson, and K. Bishop. 2007. Spatial variation in discharge and concentrations of organic carbon in a catchment network of boreal streams in northern Sweden.

Thompson, J. R., A. J. Green, and D. G. Kingston. 2014. Potential evapotranspiration-related uncertainty in climate change impacts on river flow: An assessment for the Mekong River basin. *Journal of Hydrology,* 510**:** 259-279. DOI: https://doi.org/10.1016/j.jhydrol.2013.12.010

Tipping, E., C. Woof. 1990. Humic substances in acid organic soils – Modeling their release to the soil solution in terms of humic charge. *J. Soil Sci.*41: 573-586.

Voeckler, H. M., D. M. Allen, and Y. Alila. 2014. Modeling coupled surface water-ground water processes in a small mountainous headwater catchment. *Journal of Hydrology,* 517**:** 1089-1106. DOI: 10.1016/j.jhydrol.2014.06.015

Vormoor, K., D. Lawrence, L. Schlichting, D. Wilson, and W. K. Wong. 2016. Evidence for changes in the magnitude and frequency of observed rainfall vs. snowmelt driven floods in Norway. *Journal of Hydrology,* 538**:** 33-48. DOI: 10.1016/j.jhydrol.2016.03.066

Wada, Y., I. E. M. de Graaf, and L. P. H. van Beek. 2016. High-resolution modeling of human and climate impacts on global water resources. *Journal of Advances in Modeling Earth Systems,* 8**:** 735-763. DOI: 10.1002/2015MS000618

Wallin, M. B., G. A. Weyhenmeyer, H. E. Chmiel, S. Peter, S. Sobek, D. Bastviken, and L. Klemedtsson. 2015. Temporal control on concentration, character, and export of dissolved organic carbon in two hemiboreal headwater streams draining contrasting catchments. *Journal of Geophysical Research G: Biogeosciences,* 120**:** 832-846. DOI: 10.1002/2014JG002814

Weyhenmeyer, G. A., D. Kothawala, L. J. Tranvik, M. Khalili, J. Temnerud, M. Fröberg, and E. Karltun. 2012. Selective decay of terrestrial organic carbon during transport from land to sea. *Global Change Biology,* 18**:** 349-355. DOI: 10.1111/j.1365-2486.2011.02544.x

Weyhenmeyer, G. A., R. A. Mu¨ller, M. Norman, and L. J. Tranvik. 2016. Sensitivity of freshwaters to browning in response to future climate change. *Climatic Change,* 134**:** 225-239. DOI: DOI: 10.1007/s10584-015-1514-z.

Winterdahl, M., K. Bishop, and M. Erlandsson. 2014a. Acidification, Dissolved Organic Carbon (DOC) and Climate Change. *Global Environmental Change***:** 281.

Winterdahl, M., M. Erlandsson, M. N. Futter, G. A. Weyenmeyer, and K. Bishop. 2014b. Intra-annual variability of organic carbon concentrations in running waters: Drivers along a climatic gradient. *Global Biogeochemical Cycles***:** 451. DOI: 10.1002/2013GB004770

Winterdahl, M., H. Laudon, S. W. Lyon, C. Pers, and K. Bishop. 2016. Sensitivity of stream dissolved organic carbon to temperature and discharge: Implications of future climates. *Journal of Geophysical Research: Biogeosciences,* 121**:** 126-144. DOI: DOI: 10.1002/2015JG002922.

Winterdahl, M., J. Temnerud, M. N. Futter, S. Löfgren, F. Moldan, and K. Bishop. 2011. Riparian Zone Influence on Stream Water Dissolved Organic Carbon Concentrations at the Swedish Integrated Monitoring Sites. *AMBIO,* 40**:** 920-930. DOI: 10.1007/s13280-011-0199-4

Xu, C.-Y. 2000. Modelling the effects of climate change on water resources in central Sweden. *Water Resources Management,* 14**:** 177-189.

Xu, C.-y., E. Widén, and S. Halldin. 2005. Modelling hydrological consequences of climate change—Progress and challenges. *Advances in Atmospheric Sciences,* 22**:** 789-797. DOI: 10.1007/BF02918679

Xuan, Y., A. Lamacˇova´, C. Duffy, P. Kra´m, and J. Hrusˇka. 2016. Hydrological model uncertainty due to spatial evapotranspiration estimation methods. *Computers & Geosciences,* 90**:** 90-101. DOI: DOI: 10.1016/j.cageo.2015.05.006.

APPENDIX I

Table A1. Hydrology parameter in HYPE 4.13.2 used in model set-up. If more than 1 value was used, e.g. for different soil layers, numbers are presented as a range.

Process	Parameter	Description	Units	Value			
General							
Evapotranspiration	*lp*	Threshold soil water for activation of PET	-	0.71			
	cevpam	Amplitude of sinus function that corrects potential evapotranspiration.	-	0.5			
	cevpph	phase of sinus function that corrects potential evaporation	d	45			
Temperature	*ttpi*	Half of temperature interval with mixed snow- and rainfall.	°C	1			
Recession	*rrcscorr*	Correction factor for soil recession coefficient	-	0			
	rrcs3	Slope dependent recession coefficient in the upper soil layer	d^{-1}	0.00026			
Soil dependent				**Peat soil**	**Thin soil**	**Clay soil**	**Coarse soil**
Water content	*wcfc*	Fraction of soil water available for PET (field capacity)	-	0.4	0.2	0.17-0.2	0.1
	wcwp	Wilting point as a fraction of depth	-	0.2	0.08	0.13-0.21	0.1
	wcep	Effective porosity as a fraction of depth	-	0.18	0.24	0.1-0.23	0.07
Percolation	*mperc*	Maximum percolation capacity	mm d^{-1}	15.69-8.7	54.2-97.29	39.12-79-8	9.7-21.4
Recession	*rrcs1&2*	Soil runoff recession coefficient	-	0.0006 & 0.22	0.017 & 0.62	0.04 & 0.46	0.0044 & 0.62
Surface runoff	*mactrinf*	Threshold for macro pore flow	mm d^{-1}	10	10	10	10

	mactrsm	Threshold soil water as a fraction of soil depth for macro pore flow and surface runoff	-	0.5	0.5	0.85	0.5
	macrate	Fraction of macro pore flow	-	0.1	0.1	0.3	0.1
	srrate	Fraction of surface runoff	-	0.37	0.67	0.65	0.06
Land use dependent				**Mire**	**Forest**		
Snow	*ttmp*	Threshold temperature for snowmelt	°C	0.14	0.5		
	cmlt	Degree-day factor	mm d^{-1} $°C^{-1}$	3.97	1.93		
Recession	*srrcs*	Recession coefficient for saturated surface runoff	-	0.17	0.46		
Evapotranspiration	*cevp*	Rate for basic potential evapotranspiration	mm d^{-1} $°C^{-1}$	0.61	0.19		
Frost	*frost*	Frost depth parameter	cm $°C^{-1}$	3.53	2.39		

APPENDIX II

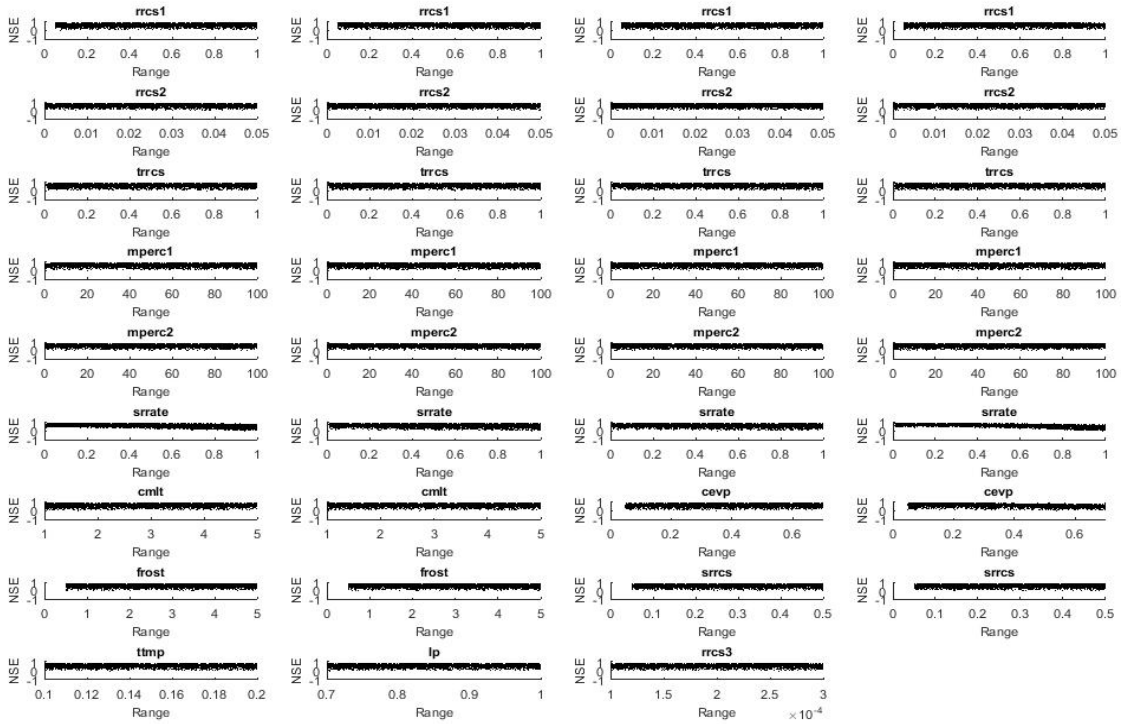

Figure A2. Sensitivity analysis performed by plotting all the range of parameter values to the corresponding NSE value resulting from the second calibration round by a Monte Carlo simulations (5000 runs). There are five soil classes and two land use classes, hence five and two figures for the same parameters. See Table 9 for the corresponding soil and land use type.

Table A2. Correlation Coefficient (CC) for the calibrated values in the second round. The five most sensitive parameters are presented in bold.

	Soil dependent					**Land use dependent**			
	Peat	Thin soil	Fine soil	Coarse soil		Mire	Forest		
	rrcs1	*rrcs1*	*rrcs1*	*rrcs1*		*cmlt*	*cmlt*	*cevp*	*cevp*
CC	0.045	-0.005	0.002	0.039	**CC**	0.037	0.004	-0.004	**-0.382**
	rrcs2	*rrcs2*	*rrcs2*	*rrcs2*		*frost*	*frost*	*srrcs*	*srrcs*
CC	-0.028	0.016	0.016	-0.013	**CC**	0.007	-0.021	0.011	0.012
	trrcs	*trrcs*	*trrcs*	*trrcs*		**General**			
CC	-0.017	0.013	-0.024	0.018		*ttmp*	*lp*	*rccs3*	
	mperc1	*mperc1*	*mperc1*	*mperc1*	**CC**	-0.004	0.04	0.024	
CC	-0.05	-0.035	-0.016	-0.045					
	mperc2	*mperc2*	*mperc2*	*mperc2*					
CC	-0.023	-0.014	-0.005	0.025					
	srrate	*srrate*	*srrate*	*srrate*					
CC	**-0.391**	**-0.129**	**-0.092**	**-0.65**					

APPENDIX III

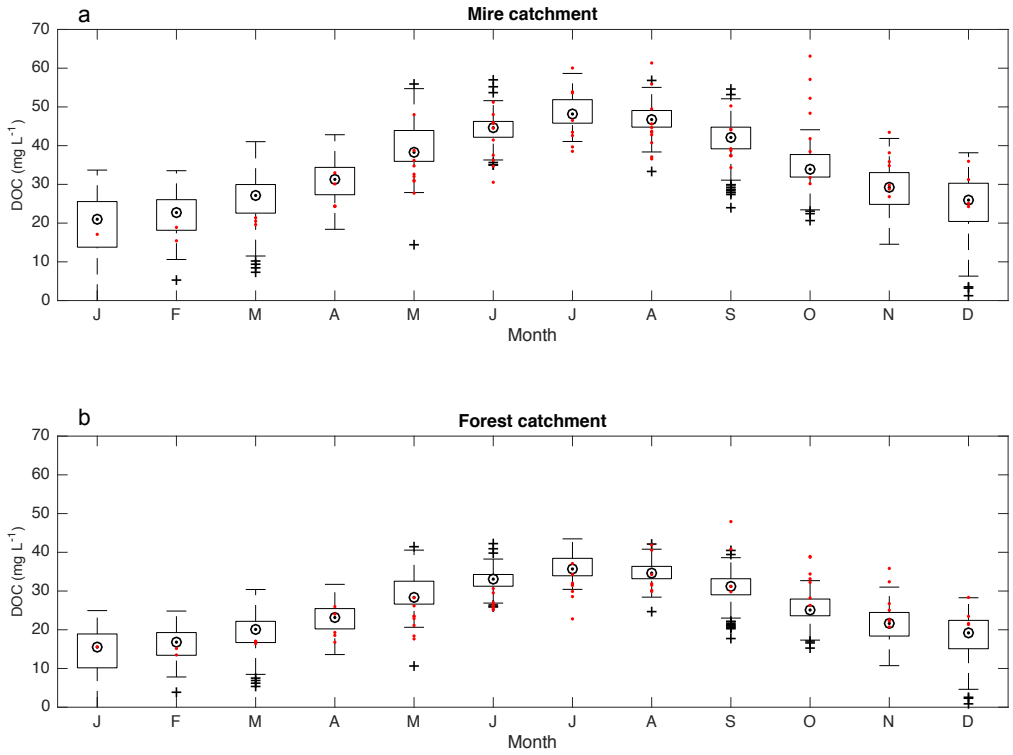

Figure A3. Modelled and observed concentrations of DOC (mg L^{-1}) for a) the mire catchment and b) the forest catchment 2012-2016. The modelled concentrations are represented by a boxplot, the box representing concentrations from the 25th percentile to the 75th percentile. Median is displayed as a black dot inside a circle. Boxplot whiskers represent 99.3% (2.7 σ) of the modelled values. Outliers are plotted as black lines. Individual measurements are presented as red dots. In total, there were 77 measured values for the mire catchment and 64 values for the forest catchment.

Institutionen för naturgeografi och ekosystemvetenskap, Lunds Universitet.
Studentexamensarbete (seminarieuppsatser). Uppsatserna finns tillgängliga på institutionens geobibliotek, Sölvegatan 12, 223 62 LUND. Serien startade 1985. Hela listan och själva uppsatserna är även tillgängliga på LUP student papers (https://lup.lub.lu.se/student-papers/search/) och via Geobiblioteket (www.geobib.lu.se)
The student thesis reports are available at the Geo-Library, Department of Physical Geography and Ecosystem Science, University of Lund, Sölvegatan 12, S-223 62 Lund, Sweden. Report series started 1985. The complete list and electronic versions are also electronic available at the LUP student papers (https://lup.lub.lu.se/student-papers/search/) and through the Geo-library (www.geobib.lu.se)

400 Sofia Sjögren (2016) Effective methods for prediction and visualization of contaminated soil volumes in 3D with GIS
401 Jayan Wijesingha (2016) Geometric quality assessment of multi-rotor unmanned aerial vehicle-borne remote sensing products for precision agriculture
402 Jenny Ahlstrand (2016) Effects of altered precipitation regimes on bryophyte carbon dynamics in a Peruvian tropical montane cloud forest
403 Peter Markus (2016) Design and development of a prototype mobile geographical information system for real-time collection and storage of traffic accident data
404 Christos Bountzouklis (2016) Monitoring of Santorini (Greece) volcano during post-unrest period (2014-2016) with interferometric time series of Sentinel-1A
405 Gea Hallen (2016) Porous asphalt as a method for reducing urban storm water runoff in Lund, Sweden
406 Marcus Rudolf (2016) Spatiotemporal reconstructions of black carbon, organic matter and heavy metals in coastal records of south-west Sweden
407 Sophie Rudbäck (2016) The spatial growth pattern and directional properties of *Dryas octopetala* on Spitsbergen, Svalbard
408 Julia Schütt (2017) Assessment of forcing mechanisms on net community production and dissolved inorganic carbon dynamics in the Southern Ocean using glider data
409 Abdalla Eltayeb A. Mohamed (2016) Mapping tree canopy cover in the semi-arid Sahel using satellite remote sensing and Google Earth imagery
410 Ying Zhou (2016) The link between secondary organic aerosol and monoterpenes at a boreal forest site
411 Matthew Corney (2016) Preparation and analysis of crowdsourced GPS bicycling data: a study of Skåne, Sweden
412 Louise Hannon Bradshaw (2017) Sweden, forests & wind storms: Developing a model to predict storm damage to forests in Kronoberg county
413 Joel D. White (2017) Shifts within the carbon cycle in response to the absence of keystone herbivore *Ovibos moschatus* in a high arctic mire
414 Kristofer Karlsson (2017) Greenhouse gas flux at a temperate peatland: a comparison of the eddy covariance method and the flux-gradient method
415 Md. Monirul Islam (2017) Tracing mangrove forest dynamics of Bangladesh using historical Landsat data
416 Bos Brendan Bos (2017) The effects of tropical cyclones on the carbon cycle
417 Martynas Cerniauskas (2017) Estimating wildfire-attributed boreal forest burn in Central and Eastern Siberia during summer of 2016
418 Caroline Hall (2017)The mass balance and equilibrium line altitude trends of glaciers in northern Sweden

419 Clara Kjällman (2017) Changing landscapes: Wetlands in the Swedish municipality Helsingborg 1820-2016
420 Raluca Munteanu (2017) The effects of changing temperature and precipitation rates on free-living soil Nematoda in Norway.
421 Neija Maegaard Elvekjær (2017) Assessing Land degradation in global drylands and possible linkages to socio-economic inequality
422 Petra Oberhollenzer, (2017) Reforestation of Alpine Grasslands in South Tyrol: Assessing spatial changes based on LANDSAT data 1986-2016
423 Femke, Pijcke (2017) Change of water surface area in northern Sweden
424 Alexandra Pongracz (2017) Modelling global Gross Primary Production using the correlation between key leaf traits
425 Marie Skogseid (2017) Climate Change in Kenya - A review of literature and evaluation of temperature and precipitation data
426 Ida Pettersson (2017) Ekologisk kompensation och habitatbanker i kommunalt planarbete
427 Denice Adlerklint (2017) Climate Change Adaptation Strategies for Urban Stormwater Management – A comparative study of municipalities in Scania
428 Johanna Andersson (2017) Using geographically weighted regression (GWR) to explore spatial variations in the relationship between public transport accessibility and car use : a case study in Lund and Malmö, Sweden
429 Elisabeth Farrington (2017) Investigating the spatial patterns and climate dependency of Tick-Borne Encephalitis in Sweden
430 David Mårtensson (2017) Modeling habitats for vascular plants using climate factors and scenarios - Decreasing presence probability for red listed plants in Scania
431 Maja Jensen (2017) Hydrology and surface water chemistry in a small forested catchment : which factors influence surface water acidity?
432 Iris Behrens (2017) Watershed delineation for runoff estimations to culverts in the Swedish road network : a comparison between two GIS based hydrological modelling methods and a manually delineated watershed
433 Jenny Hansson (2017) Identifying large-scale land acquisitions and their agro-ecological consequences : a remote sensing based study in Ghana
434 Linn Gardell (2017) Skyddande, bevarande och skapande av urbana ekosystemtjänster i svenska kommuner
435 Johanna Andersson (2017) Utvärdering av modellerad solinstrålning i södra Sverige med Points Solar Radiation i ArcGIS
436 Huiting Huang (2017) Estimating area of vector polygons on spherical and ellipsoidal earth models with application in estimating regional carbon flows
437 Leif Holmquist (2017) Spatial runner: environmental and musical exposure effects on runners through an idealized routing network
438 Adriana Bota (2017) Methodology for creating historical land use databases – a case study for ICOS-station Hyltemossa, Sweden
439 Michael Araya Ghebremariam (2017) Urban flood modelling: a GIS based approach in Lomma, Skåne region
440 Stina Sandgren (2017) Climate change impact on water balance and export of dissolved organic carbon – a sub-catchment modeling approach